The Economic Case for Global Vaccinations: An Epidemiological Model with International Production Networks*

Cem Çakmaklı[†] **Selva Demiralp**[‡] **Şebnem Kalemli Özcan**[§]
Sevcan Yeşiltaş[¶] **Muhammed A. Yıldırım**[||]

September 2025

Abstract

We present a global general equilibrium model that incorporates input-output linkages across multiple sectors and countries to analyze the impact of pandemic-related labor supply shocks. These shocks vary across industries due to differences in how occupations are affected by the disease, influenced by factors such as contact intensity and the feasibility of remote work. Using the model, we quantify the economic rationale for global vaccinations. Given empirically relevant trade and production elasticities, where labor and imported intermediate inputs complement each other, we examine several scenarios. If wealthy countries vaccinate only their own populations, global output could decline by nearly 1% compared to pre-pandemic levels. In contrast, investing in global vaccinations could yield a 178% return on investment for wealthy nations and potentially halve the global output decline. Vaccinating low-income countries could mitigate economic impacts on wealthy nations through sectoral trade and production linkages, significantly reducing losses by 70% without compromising rich countries own vaccination efforts.

Keywords: Sectoral Shocks; Production Networks; International Linkages.

JEL Codes: C67, D57, F00, F16, F17, I18, P45.

*We are privileged to have received late Emmanuel Farhi's feedback on earlier drafts. We thank David Baqaee, Nitya Pandalai-Nayar and Alvaro Silva for their insightful comments. We thank Yasin Şimşek for excellent research assistance and Ayşe Nur Demiralp for the quote in the preamble. We thank seminar participants at NBER, IMF, ECB, CEPR, EIB, Central Bank of Chile, OECD, the World Bank, and the Koç University-TUSIAD Economic Research Forum for their comments. We acknowledge support from the ICC Research Foundation.

[†]Durham University and Koç University.

[‡]Koç University.

[§]Brown University, NBER and CEPR.

[¶]Koç University.

[||]The Growth Lab at Harvard University and Koç University

No Man is an Island
"No man is an island entire of itself; every man is a piece of the continent, a part of the main; if a clod be washed away by the sea, Europe is the less, as well as if a promontory were, as well as any manner of thy friends or of thine own were; any man's death diminishes me, because I am involved in mankind. And therefore never send to know for whom the bell tolls; it tolls for thee."

– John Donne

1 Introduction

On January 28, 2021, Taiwan reached out to Germany for assistance in obtaining Covid-19 vaccines, following Berlin's request for help with a shortage of automobile semiconductor chips.[1] This initiative by Taiwan represented a strategic maneuver to address two critical shortages simultaneously: the scarcity of vaccines and semiconductor chips. In exchange for chips vital to its automobile industry, Germany was expected to provide sufficient vaccines to curb the pandemic in Taiwan, thereby ensuring the continued production and delivery of chips to Germany.

Within a year, these shortages had extended to other sectors, impacting all factors of production. Our study employs a multi-sector-country framework to quantify the sector-specific output losses attributed to these shortages, which arise from imbalances in the supply of factors of production across sectors and asymmetric consumer demand for goods from different sectors. With our open economy model, we also assess the relative decline in domestic expenditures across countries and evaluate the resulting welfare loss. In our analysis, pandemic-related shocks to sectoral demand and supply can only be alleviated through global vaccinations. Due to the uneven pace of vaccinations globally, these shocks propagate through supply chains from countries with low vaccination rates to those with higher rates. We estimate the hypothetical changes in global and national-level output under various scenarios by comparing outcomes with and without access to vaccines that are enough to vaccinate a sizeable share of the population.

Our key findings are as follows: Using empirically relevant trade and production elasticities, we determine that if wealthy countries only vaccinate their own populations, global output decreases by nearly 1% compared to pre-pandemic levels, with the wealthy nations bearing 15% of this global loss. Conversely, if wealthy countries allocate vaccines equivalent to 50% of their populations to low-income countries (a feasible amount considering

[1] https://www.reuters.com/article/us-health-coronavirus-taiwan-idINKBN29X11P.

that wealthy nations initially stockpiled vaccines equal to three times their populations), this could immunize a third of the global poor within less than 8 months. This strategy yields a 178% return on investment for wealthy countries and reduces global output losses by half, thereby decreasing the wealthy countries' share of the global loss to 9%.[2] It's important to note that under this scenario, rich countries can still vaccinate 100% of their populations. Consequently, the losses incurred by rich countries decrease by 70% solely due to enhanced trade and production connections with low-income countries, as their investment resolves supply chain bottlenecks. This underscores the economic rationale for global vaccinations. In another hypothetical scenario that tries to come close to actual vaccine distribution, where half of the population in low-income countries is vaccinated by the end of 2021, the global loss decreases by 12% (instead of halving), and losses for rich countries increase by 60% compared to the previous scenario where low-income countries were vaccinated more rapidly and extensively.[3]

Our framework builds upon the closed-economy model introduced in Baqaee and Farhi (2022). By extending it to a global context, we model the transmission of demand and supply shocks through global supply chains. The primary empirical contribution of our study is to quantify the economic losses experienced by vaccinated countries due to deficiencies in vaccination rates in other nations, which propagate shocks through global linkages. For instance, the zero-Covid strategies adopted by unvaccinated trading partners manifest as new sectoral shocks in vaccinated countries, echoing the findings of Guerrieri et al. (2022) where a supply shock in one sector can lead to a demand shock in another. The sole friction in our model lies in segmented labor markets, implying that labor supply is specific to sectors and not mobile across sectors within any given country.[4] Labor demand in our model adjusts endogenously to exogenous consumption shocks, such as shifts in consumer preferences from services to goods. Our model does not include nominal rigidities; therefore, sectoral wages adjust freely to achieve equilibrium within each sector, reflecting a segmented labor market.

Our two-period model is calibrated as follows: The primary shock is a sectoral labor supply shock, approximated by sector-specific infections. The first period represents the

[2]The 178% return rate is derived by comparing our estimated expenditure losses of 338 billion USD with the projected 190 billion USD cost to manufacture sufficient vaccines for global inoculation. This cost projection is based on COVAX's early 2021 estimate of 38 billion USD to produce enough vaccine doses to immunize the world's vulnerable population.

[3]Our analysis focuses on 2021, and as of August 2022, a third of the world remained unvaccinated. See https://ourworldindata.org/covid-vaccinations.

[4]According to Fernald and Li (2022), there was no significant labor reallocation across sectors in the U.S. during the pandemic.

pre-Covid-19 equilibrium, while the second period simulates the pandemic by integrating sectoral shocks. Within our calibration framework, the duration of the second period dictates when the economy reverts to the pre-Covid-19 equilibrium. We divide the second period into 365 days and solve the model daily. Daily sectoral shocks are determined by the day-to-day dynamics of the disease, modeled using epidemiological parameters established at the onset of vaccine discovery. Additionally, our model incorporates endogenous lockdowns: When the number of infected individuals exceeds a country's ICU bed capacity—a threshold derived from empirical data—we initiate a lockdown. It's important to note that sectoral labor supply shocks occur daily based on the number of individuals unable to work due to illness and the rate of vaccination. Once a country achieves full vaccination coverage, sectoral shocks cease, and the model returns to its pre-pandemic equilibrium. Thus, the conclusion of the second period is contingent upon the vaccination scenarios and the occurrence of endogenous lockdowns.

How do we get sectoral infections from an epidemiological model? Starting with the pre-pandemic employment baseline for each sector-country pair, we introduce infection-driven demand and supply shocks to assess deviations from this equilibrium. The magnitude of labor supply shocks is influenced by contact intensity within the sector, the feasibility of remote work, and the imposition of lockdowns. Thus, each country-sector pair receives its own sectoral labor supply shock. Additionally, we model a sectoral demand shifter to reflect compositional changes in consumption from services to goods. To calibrate these sectoral shifts, we utilize data on personal consumption expenditures by sector for the U.S. economy. From this data, we derive the relationship between sectoral changes in consumption and sectoral infections for the U.S. Subsequently, we extend these projections to the other 64 countries in our study, applying the parameters obtained from the U.S. data and using country-level infection rates.

We start with the pre-pandemic equilibrium and calibrate the global linkages to OECD's Inter-Country Input-Output (ICIO) tables,[5] as depicted in Figure 1a and Figure 1b. Of the 65 countries analyzed, 39 are classified as advanced economies (AEs) with access to vaccines as of January 2021, while the remaining countries—including a collective entity labeled the "Rest of the World"—are categorized as emerging markets and developing economies (EMDEs) and are presumed unvaccinated at the start.

[5]As of the time of this writing, the OECD had not updated its global network data to reflect changes in network expenditure changes during the pandemic, therefore, we used the data from the latest available year of 2015. Anecdotal evidence suggests shipping delays and inventory adjustments throughout 2021, but this information alone is inadequate for calculating endogenous changes in the global network's expenditure shares.

Figure 1: Inter-country Inter-industry Trade Linkages

(a) International Trade Linkages

(b) Inter-industry Trade Linkages

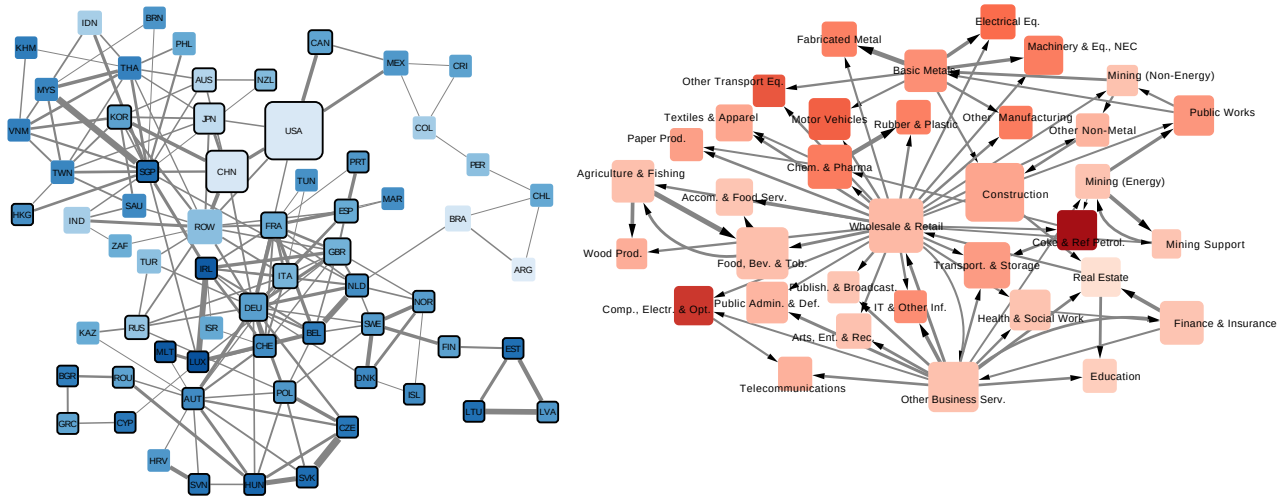

NOTES: Panel (a) presents a summary of international linkages. Each node corresponds to a country, with sizes proportional to the GDP of the respective country. The node color indicates the country's openness, defined as the ratio of imports and exports to GDP, with darker shades signifying higher trade openness (See Table E.1). Countries with vaccine access are highlighted by black borders. The thickness of the lines between nodes increases with the volume of bilateral trade. For expositional clarity, we only show the top two significant trade relations per country for 65 countries in our dataset. Panel (b) illustrates aggregated inter-industry linkages. Each node represents an industry, with node size reflecting the industry's total intermediate usage. The smallest node, representing the Mining Support industry, corresponds to 184 billion USD, while the largest, for the Construction industry, corresponds to 5.9 trillion USD. Node colors indicate the proportion of imported inputs, ranging from 5.9% in the Real Estate industry to 37% in the Coke & Refined Petroleum industry. The thickness of edges from the supplying to the target industry indicates the strength of trade relations, based on two criteria: (i) the intermediate input from the supplier constitutes at least 10 percent of the inputs of the target industry, or (ii) the supplier ranks among the top two suppliers of the target industry. The network displays 35 nodes and 72 edges. Source: ICIO Tables for 2015 OECD (2020).

In our baseline calibration, we employ estimated trade elasticities from Boehm et al. (2019, 2023), which are relatively low. For robustness, we also use higher elasticities from Caliendo and Parro (2015) to reflect greater substitution possibilities. Low elasticities imply complementarity between domestic and foreign inputs, resulting in higher estimated losses since, in the short run, countries cannot easily replace their imported intermediate inputs from one source with those from another. An open economy, though more integrated into the global production network and thus more vulnerable to supply-chain shocks, is also beneficial in terms of larger number of suppliers. Thus, using higher elasticities allows for medium-to-long-run substitution between suppliers. We have the interesting result that, under complementarity, AEs account for a smaller share of the global loss since EMDEs, unable to produce without foreign inputs, bear a larger portion of the loss. Conversely, with high substitution elasticities, EMDEs are much better off and, hence, AEs account for

a larger share of the global output loss. Given the importance of supply chains for EMDEs, substitution benefits them more as long as they get to be vaccinated.

The structure of this paper is as follows. Section 2 introduces our model. Section 3 details the data and parameters used for calibration. In Section 4, we discuss the findings of our quantitative analysis and examine the robustness of these results. Section 5 provides concluding remarks.

2 The Model

Our model analyzes the transmission of sectoral supply and demand shocks within the production network and hence we deliberately exclude aggregate shocks and nominal rigidities to focus on the sectoral dynamics. We solve the analytical model using small perturbations/shocks that provide an exact hat-algebra solution, rather than solving the model via log-linearization around the steady state. This solution method is similar to Baqaee and Farhi (2024), who focus on different shocks, namely tariff changes. This approach allows us to integrate responses to many successive small shocks, thereby accommodating relatively large shocks as well. The difference of our method is that we hard code all different types of Allen-Uzawa elasticities into our computations, which reduces the time needed for a full solution at each perturbation stage.

Our two-period model runs intra-temporally within each period. Across the two periods, consumption adjusts in response to sectoral shocks. However, due to the absence of an aggregate demand shock, there is effectively no intertemporal aspect and, hence, consumers act as hand-to-mouth agents who spend their income within each respective period.

2.1 Environment

Notation. Each country produces and consumes final and intermediate goods and services. We denote the set of countries with $\mathcal{C}$ and we index countries with c, v or m. The $\mathcal{N}$ denotes the set of industries or sectors (we use these terms interchangeably) that are indexed by i, j or k. A sector i in country c is denoted by ic and we denote the set of all such pairs with $\mathcal{CN}$. Production in ic can use inputs from sector j in country m, i.e., jm. For example automotive industry, i, in Germany, c, imports steel, j, from country m, Turkey. For convenience, we also introduce the consumption as sector $0 \notin \mathcal{N}$, and consumption in country c is indexed by $0c$. The set of factors is represented by $\mathcal{F}$ and indexed by f or g. Because we work with more than 2 countries, more than 2 sectors, and more than 2 factors, this notation is essential. We denote the set of factors present and owned by country c with $\mathcal{F}_c$.

Prices, outputs and expenditures. The output of industry i in country c is denoted with y_{ic} and its price with p_{ic}. The country-sector pair ic uses inputs from other sectors from different countries in addition to labor. We show the inputs used from sector j in country m by sector i in country c with x_{jm}^{ic} and the price of this input is p_{jm}.[6] Recall that $i = 0$ denotes the consumption of households. We assume $y_{0c} = C_c$ is the total consumption in country c and the price index of consumption is denoted by p_{0c}. Let's denote the total nominal expenditure of country c with $E_c = p_{0c}y_{0c} = p_{0c}C_c$. The total world expenditure is $E \equiv \sum_c E_c$, which is also equal to the total world GDP. We assume that the factors are country and sector-specific. Since they are sector-specific, with an abuse of notation, we use industry indices to address them as well. For any factor used by industry i in country c, we denote the corresponding labor with L_{ic} and its wage with w_{ic}.

Input-Output Matrix. We use expenditure shares for both the consumption and the production sides of the economy to construct the input-output matrix. The input share of sector j of country m in sector i in country c is defined by:

$$\Omega_{jm}^{ic} \equiv \frac{p_{jm}x_{jm}^{ic}}{p_{ic}y_{ic}}. \tag{1}$$

We denote the input share matrix with $\Omega^{\mathcal{N}}$. We express the expenditure share of industry jm in final good consumption in country c as:

$$\Omega_{jm}^{0c} \equiv \frac{p_{jm}x_{jm}^{0c}}{E_c}, \tag{2}$$

where x_{jm}^{0c} denotes the amount of industry jm's output consumed by the households in country c. The matrix corresponding to the final consumption is denoted by Ω^0. Finally, the value-added (or factor share) in country-sector pair ic is defined as:

$$\alpha_{ic} \equiv \Omega_{ic}^{\mathcal{F}} \equiv \frac{w_{ic}L_{ic}}{p_{ic}y_{ic}} = 1 - \sum_{jm \in \mathcal{CN}} \Omega_{jm}^{ic}. \tag{3}$$

Note that $\Omega^{\mathcal{F}}$– the matrix representing the factor shares– corresponds to a diagonal matrix whose elements are given by the value-added share.

[6] We solve the changes in the log prices and quantities to implement hat algebra used in the trade literature (Costinot and Rodríguez-Clare, 2014; Caliendo and Parro, 2015). We assume that the trade costs, specifically tariffs, do not change during the pandemic. The increase in shipping costs enters into the model because the transportation sector is represented as a separate entry in the Input-Output matrix. In the model, we initialize the price of each good to be 1 in each country. Hence, when we solve for log-changes, price changes for a given variety are the same in each country.

2.2 Production

Figure 2 summarizes our production side. Production in each sector i in country c is achieved by combining sector-specific labor and a bundle of intermediate inputs. The assumption of sector-specific labor implies that labor is not mobile between sectors but can fluctuate within a sector over time. The empirical evidence during the pandemic supports the presence of within-sector reallocation and the absence of between-sector reallocation as shown by Fernald and Li (2022). The intermediate bundle for a sector-country pair ic consists of all the inputs from different sector bundles. These sector bundles, in turn, are formed by different sector-country varieties.

Figure 2: Production Structure

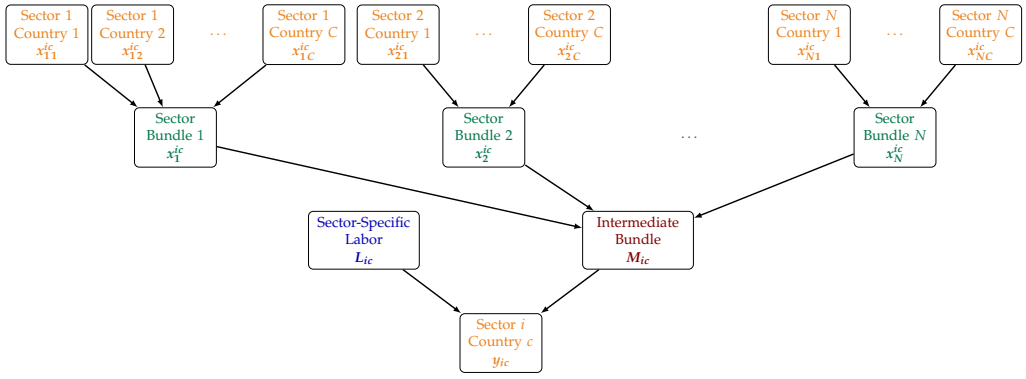

NOTES: This figure presents the inputs used in the production for sector i in country c. All the aggregations are done with functions exhibiting constant elasticity of substitution, albeit with different elasticities. Sector varieties, sector bundles, intermediate bundles, and labor are all country-sector specific. We show the notation that we use for each input in the last line of each box.

Let's explain this production structure with an example from German automotive manufacturing. German automobiles are produced by German workers and an intermediate bundle. This intermediate bundle consists of sector bundles such as steel, plastic, textiles, leather, and glass. These sector bundles are aggregates of sector varieties from different countries. The steel bundle for German automotive manufacturing, for instance, is formed by steel from Turkey, India, China, the U.S., etc. We assume that the production follows this three-layer nested CES structure as shown in Figure 2. Next, we formalize each of these steps and highlight the key parameters.

The production in country-sector pair ic is achieved by combining the sector-specific labor and the intermediate bundle. We denote the price of this bundle with p_M^{ic} and its quantity with M_{ic}. We assume that the production of the final good follows a constant elasticity of substitution (CES) technology with elasticity ϕ. The production function for

the firms is given by:

$$y_{ic} = A_{ic}\left[\alpha_{ic}^{1/\phi} L_{ic}^{\frac{\phi-1}{\phi}} + (1-\alpha_{ic})^{1/\phi} M_{ic}^{\frac{\phi-1}{\phi}}\right]^{\frac{\phi}{\phi-1}}. \tag{4}$$

where A_{ic} is the productivity.[7] The corresponding price index is:

$$p_{ic} = \frac{1}{A_{ic}}\left[\alpha_{ic}\left(w_{ic}\right)^{1-\phi} + (1-\alpha_{ic})\left(p_M^{ic}\right)^{1-\phi}\right]^{\frac{1}{1-\phi}}.$$

We assume $0 \leq \phi < 1$, i.e., labor and intermediate inputs are complements. As we show in the calibration section, this assumption is supported by the estimates we use from the empirical literature.

The intermediate bundle in ic is composed of inputs of sectoral bundles, denoted by x_j^{ic} for sector j. Assuming a CES aggregator with elasticity of substitution of ε, the intermediate bundle, M_{ic}, and its price index is given by:

$$\Omega s_j^{ic} \equiv \sum_{m\in\mathcal{C}} \Omega_{jm}^{ic}, \qquad M_{ic} = \left[\sum_{j\in\mathcal{N}} \left(\frac{\Omega s_j^{ic}}{1-\alpha_{ic}}\right)^{1/\varepsilon} \left(x_j^{ic}\right)^{\frac{\varepsilon-1}{\varepsilon}}\right]^{\frac{\varepsilon}{\varepsilon-1}}, \quad p_M^{ic} = \left[\sum_{j\in\mathcal{N}} \frac{\Omega s_j^{ic}}{1-\alpha_{ic}} \left(p_j^{ic}\right)^{1-\varepsilon}\right]^{\frac{1}{1-\varepsilon}}.$$

Ωs_j^{ic} captures the share of sector j in production of ic and is calculated by summing over the country varieties. p_j^{ic} is the sectoral price index. We assume that $0 \leq \varepsilon < 1$, i.e., all sectoral inputs for the intermediate bundle are complements. This assumption implies that plastic and steel cannot be easily substituted in auto production, which is backed by the estimates from the empirical literature, as we show in our calibration section.

Sector bundles are aggregates of varieties coming from different countries. We capture

[7] To ensure the model's completeness, we include the sectoral productivity term. However, we do not introduce any productivity shocks in our calculations. Another formulation for this equation is to use the calibrated CES representation:

$$y_{ic} = \frac{A_{ic}}{\bar{A}_{ic}}\left[\alpha_{ic}\left(\frac{L_{ic}}{\bar{L}_{ic}}\right)^{\frac{\phi-1}{\phi}} + (1-\alpha_{ic})\left(\frac{M_{ic}}{\bar{M}_{ic}}\right)^{\frac{\phi-1}{\phi}}\right]^{\frac{\phi}{\phi-1}},$$

where the values with a bar on top denote the pre-pandemic 2019 equilibrium normalization. With this calibrated formulation, and by selecting appropriate normalizations, we can assume all prices and productivity parameters are equal to 1 in the pre-shock state. Our solution methodology involves approximating large shocks by introducing small shocks across multiple iterations. At each iteration, we recalibrate the model, ensuring that the weights in the primitive CES functions correspond to the input shares. In all the CES functions below, we can rewrite them as their calibrated versions as well.

the share of bundle j for sector ic fulfilled by jm with the matrix $\Xi^{\mathcal{N}}$, and write the sectoral bundle input and the price index as:

$$\Xi_{jm}^{ic} \equiv \frac{\Omega_{jm}^{ic}}{\Omega s_j^{ic}}, \qquad x_j^{ic} = \left[\sum_{m\in\mathcal{C}} \left(\Xi_{jm}^{ic}\right)^{1/\xi_j} \left(x_{jm}^{ic}\right)^{\frac{\xi_j-1}{\xi_j}}\right]^{\frac{\xi_j}{\xi_j-1}}, \qquad p_j^{ic} = \left[\sum_{m\in\mathcal{C}} \Xi_{jm}^{ic} \left(p_{jm}\right)^{1-\xi_j}\right]^{\frac{1}{1-\xi_j}},$$

This uses a CES aggregator with a sector-specific elasticity of substitution ξ_j. These sector-specific elasticities are estimated to allow substitutions between varieties coming from different countries in the long term (Costinot and Rodríguez-Clare, 2014; Caliendo and Parro, 2015) such that $\xi_j \geq 1$. But in the short term, we assume that it is hard to immediately substitute varieties from different countries to capture what happened during the pandemic. The case of $\xi_j \leq 1$ is estimated by Boehm et al. (2019). Our empirical exercise presents results for the cases of low and high substitution, for the range of $\xi_j \leq 1$ & $\xi_j \geq 1$.

2.3 Consumption

There is a representative agent in each country solving a two-period consumption optimization problem. The first period corresponds to the pre-pandemic stage and the second period corresponds to the pandemic stage. The households collect their income through factor ownership. Each period, the national expenditure is equal to $E_{c,t}$. We normalize the world expenditure to 1 in both periods. In the absence of aggregate shocks and perfect foresight, the model effectively solved for each period. Hence, we drop the time subscript below to simplify the notation.

Figure 3: Consumption Structure

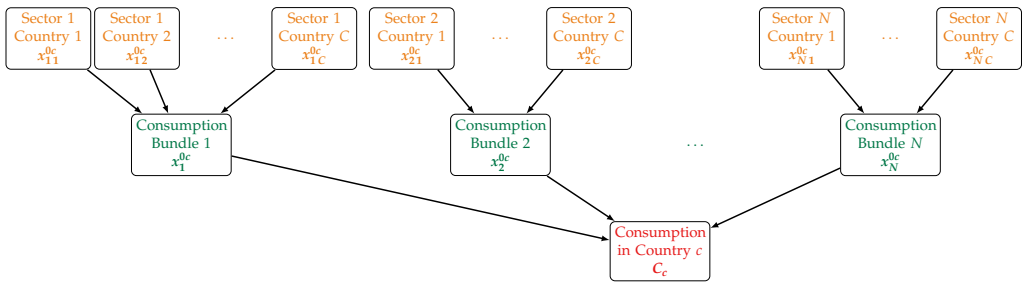

NOTES: This figure presents the consumption choice in country c. All the aggregations are done with functions exhibiting constant elasticity of substitution albeit with different elasticities. The consumption bundles are country-specific.

Similar to our production structure, we also assume a nested structure in consumption

as depicted in Figure 3. The representative agent optimization is given by:

$$C_c = \left[\sum_{j \in \mathcal{N}} \left(\Omega s_j^{0c} \right)^{1/\sigma} \left(x_j^{0c} \right)^{\frac{\sigma-1}{\sigma}} \right]^{\frac{\sigma}{\sigma-1}}, \quad \text{with} \quad \Omega s_j^{0c} \equiv \sum_{m \in \mathcal{C}} \Omega_{jm}^{0c}$$

where x_j^{0c} denotes the (normalized) sectoral consumption and Ωs_j^{0c}denotes the share of industry j in the final consumption of consumers in country c. We assume σ to be equal to 1 for Cobb-Douglas preferences. Similar to the production side, consumption bundles that are comprised of varieties from different countries. The corresponding consumption price index can be written as:

$$p_{0c} = \left[\sum_{j \in \mathcal{N}} \Omega s_j^{0c} \left(p_j^{0c} \right)^{1-\sigma} \right]^{\frac{1}{1-\sigma}}, \quad \text{for } (\sigma = 1) : \log p_{0c} = \sum_{j \in \mathcal{N}} \Omega s_j^{0c} \log p_j^{0c}, \tag{5}$$

where p_j^{0c} denotes the price of the consumption bundle j in country c, $\sigma = 1$ corresponds to the Cobb-Douglas case with constant expenditure shares.

We capture the share of bundle j for consumers in c fulfilled by jm with the matrix Ξ^0, and write the sectoral consumption bundle and its price index as:

$$\Xi_{jm}^{0c} \equiv \frac{\Omega_{jm}^{0c}}{\Omega s_j^{0c}}, \qquad x_j^{0c} = \left[\sum_{j \in \mathcal{N}} \left(\Xi_{jm}^{0c} \right)^{1/\xi_j^0} \left(x_{jm}^{0c} \right)^{\frac{\xi_j^0 - 1}{\xi_j^0}} \right]^{\frac{\xi_j^0}{\xi_j^0 - 1}}, \qquad p_j^{0c} = \left[\sum_{m \in \mathcal{C}} \Xi_{jm}^{0c} \left(p_{jm} \right)^{1-\xi_j^0} \right]^{\frac{1}{1-\xi_j^0}}.$$

As in the production side, ξ_i^0 is the trade elasticity for consumption. We use values both from Caliendo and Parro (2015) and from Boehm et al. (2023), so we study cases where these elasticities are greater and smaller than 1.

2.4 Equilibrium and Perturbation

Given the parameters, a general equilibrium consists of good prices, factor prices, outputs, intermediate inputs, factor inputs, and consumption levels such that producers minimize their costs, households maximize their utilities, and good and factor markets clear. The equilibrium is stable in the absence of any shocks. We perturb this equilibrium with sectoral demand and supply shocks. At each point in time, we assume that good markets clear such

that for any industry ic:

$$y_{ic} = \sum_{m \in \mathcal{C}} \sum_{j \in \mathcal{N}} x_{ic}^{jm} + \sum_{m \in \mathcal{C}} x_{ic}^{0m}. \tag{6}$$

The first term corresponds to the intermediate input usage of ic by all country-industry pairs, indexed by jm. The second term captures to the final good usage of ic in all countries, indexed by m. We also assume labor markets clear such that all "potential" sector-specific workers are employed.

At the initial equilibrium, we set all prices to 1 and all output of country-sector pairs to their respective share in the total nominal world expenditure. After perturbing with shocks, the prices and outputs re-equilibriate.

2.5 Domar Weights, GDP and Country-Level Expenditures

Let's define the Domar weight of an industry ic to be: $\lambda_{ic} \equiv p_{ic} y_{ic} / E$ and for the factor employed in the same industry to be $\Lambda_{ic} \equiv w_{ic} L_{ic} / E$. We denote the expenditure share of country m with $\chi_m \equiv E_m / E$. Starting from market clearing condition in Equation (6), using the expenditures for each country, E_c, we can write the sector Domar weight for ic as:

$$\lambda_{ic} \equiv \frac{p_{ic} y_{ic}}{E} = \sum_{m \in \mathcal{C}} \frac{p_{ic} x_{ic}^{0m}}{E_m} \frac{E_m}{E} + \sum_{jm \in \mathcal{CN}} \frac{p_{ic} x_{ic}^{jm}}{E} = \sum_{m \in \mathcal{C}} \Omega_{jm}^{0c} \chi_m + \sum_{jm \in \mathcal{CN}} \Omega_{kc}^{jm} \lambda_{jm}. \tag{7}$$

Let λ and χ denote the row-vectors corresponding to the Domar weights of sectors and expenditure shares of countries, respectively. Then, Equation (7) can be written as:

$$\lambda = \chi \Omega^0 + \lambda \Omega^{\mathcal{N}} \Rightarrow \lambda = \chi \, \Omega^0 \underbrace{(I - \Omega^{\mathcal{N}})^{-1}}_{\equiv \Psi^{\mathcal{N}}} = \chi \, \Omega^0 \, \Psi^{\mathcal{N}}, \tag{8}$$

where $\Psi^{\mathcal{N}}$ is the Leontief Inverse. The row vector for factor Domar weights, denoted by Λ, captures the ratio of added value to the world GDP in each sector. We can write it as:

$$\Lambda = \lambda \, \Omega^{\mathcal{F}} = \chi \, \Omega^0 \underbrace{\Psi^{\mathcal{N}} \, \Omega^{\mathcal{F}}}_{\equiv \Psi^{\mathcal{F}}} = \chi \, \Omega^0 \, \Psi^{\mathcal{F}}. \tag{9}$$

The total world output (GDP) is the same as total world expenditure (GNE) and we normalize them to be equal to 1. For a country c, its output (GDP), denoted as Π_c, corresponds to the total value-added in the country. Hence, we can write this country's GDP in terms of

its factor Domar weights as:

$$\Pi_c \equiv \sum_{f \in \mathcal{F}_c} \Lambda_f \qquad \Rightarrow \qquad \Pi = \Lambda \, \Phi^G. \tag{10}$$

where Φ^G is the matrix that assigns factors to countries with, Φ^G_{fc} equal to 1 if $f \in \mathcal{F}_c$ and 0 otherwise. Consistent with the real world, we allow countries to run trade surpluses or deficits, similar to Dekle et al. (2007); Costinot and Rodríguez-Clare (2014). First, we define the trade balance of country c with $\text{TB}_c \equiv \Pi_c - \chi_c$, where χ_c denotes country's expenditure (GNE). TB could be positive for a trade surplus or negative for a trade deficit. Trade deficit corresponds to the current account balance in our model. Because there is no acquisition of assets in international capital markets by assumption, the current account deficit is financed only by "net factor income from abroad (NFIA)". We calibrate the NFIA term by using data from initial current account balances in 2019.

Using the definition of GDP in terms of factors and assuming that the GDP claims of each country on other countries is proportionally distributed to their factor income assignment, we can write country nominal expenditures as (GNE), χ:

$$\chi = \Pi + \mathbf{TB} = \Lambda \, \Phi^G + \mathbf{TB}. \tag{11}$$

The second equality follows from Equation (10). We calibrate **TB** vector to the pre-pandemic trade balances from 2019 and the initial factor Domar weights from ICIO tables that are sector-country level. Once we shock this initial equilibrium, the factor Domar weights (Λ) are endogenously solved, hence the country-level expenditure, χ, endogenously adjust after the shocks. Hence, current accounts also endogenously adjust through factor income changes as factors assigned to countries change via Φ^G.

2.6 Shocks

Sectoral Supply Shocks. We start with shocks to "potential" labor supply. People may not necessarily die, but they still cannot go to work either because they are sick, or taking care of sick, or their workplace is not safe, or their employers operate under other restrictions. All these factors will have negative effects on labor supply, making the economy operate inside the production possibilities frontier. The production in the given country-sector pair ic changes as a response to the labor supply shock specific to that pair, denoted by $\Delta^L_{ic}(I_{c,t})$,

which depends on the infection level in country c at time t. Hence, Equation (4) changes to:

$$y_{ic,t} = A_{ic}\left[\alpha_{ic}^{1/\phi}\left(\Delta_{ic}^{L}(I_{c,t})L_{ic}\right)^{\frac{\phi-1}{\phi}} + (1-\alpha_{ic})^{1/\phi} M_{ic}^{\frac{\phi-1}{\phi}}\right]^{\frac{\phi}{\phi-1}}. \tag{12}$$

Sectoral Demand Shocks. On the consumption side, it is well known that sectoral consumption shifted from services to goods in the early phase of the pandemic and started shifting back slowly during the recovery phase (e.g., see Figure 7a for the U.S.). di Giovanni et al. (2022) documented different timing of such compositional changes in consumption across several countries. Chetty et al. (2020) emphasizes that the fear of contracting the disease is the main source of the decline in spending at the initial stages of the pandemic in contact-intensive sectors. Similarly, using cell phone data to track the movements of individuals, Goolsbee and Syverson (2021) show that even though the consumer traffic fell by 60%, only 7% could be explained by the lockdown suggesting that changes in consumer behavior are most likely driven by the fear of infection. We model this as a sectoral demand shifter, $\Delta_j^{0c}(I_{c,t})$, which in turn is a function of infection levels. Thus, Equation (5) changes to:

$$p_{0c,t} = \left[\sum_{j\in\mathcal{N}}\left(\Delta_j^{0c}(I_{c,t})\right)^{\sigma}\Omega s_j^{0c}\left(p_j^{0c,t}\right)^{1-\sigma}\right]^{\frac{1}{1-\sigma}}, \text{with } \sum_{j\in\mathcal{N}}\left(\Delta_j^{0c}(I_{c,t})\right)^{\sigma}\Omega s_j^{0c} = 1. \tag{13}$$

SIR Model for Sectoral Infections. Figure 4 summarizes how we combine our model with an epidemiological framework. The bottom half of the figure describes the supply side and the top half depicts the demand side. On the supply side, the transmission dynamics of the virus would differ depending on whether the workers are on-site or at a remote location like home. Among the professions that need to be carried out on the work site, we assume that the viral transmission depends on the physical proximity between the workers or between the workers and the customers. An on-site worker could be exposed to infection either at work or outside work. Production is affected by domestic labor supply shocks linked to infections. Imported inputs are affected by the evolution of the pandemic in other countries. On the demand side, both domestic and foreign demand for final and intermediate goods change with consumer preferences depending on the infection levels at home and in foreign countries.

The outcomes of the SIR model determine the dynamic trajectory of the pandemic, which is directly integrated into our framework. Specifically, sectoral consumption shocks,

Figure 4: Integrating the Economic and SIR Models

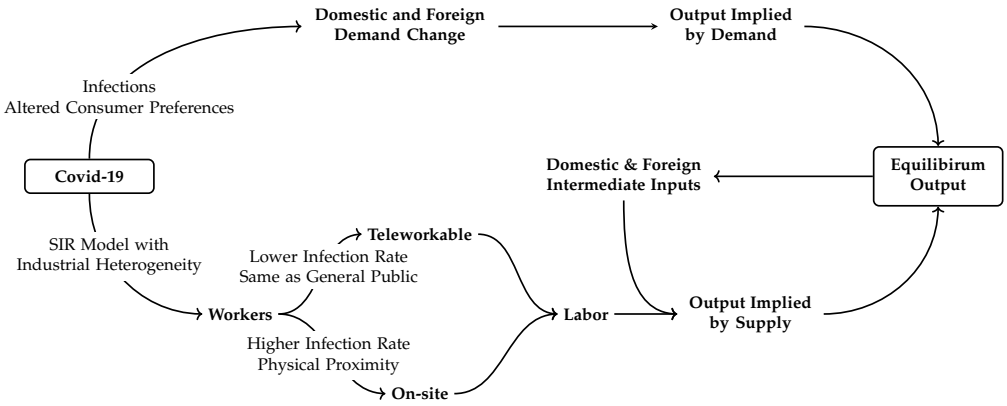

denoted by $\Delta^{0c} j(Ic,t)$, are a function of the aggregate infection level within each country. In contrast, sectoral labor supply shocks, $\Delta^{L}_{ic}(Ic,t)$, depend on sector-specific infection rates. These rates can differ across sectors due to the heterogeneous transmission dynamics captured by our sector-specific SIR framework, as described in Appendix A. Vaccination plays a critical role in shaping the course of the pandemic by moving individuals directly from the susceptible group to the recovered group, thereby circumventing the infection phase. We incorporate these time-varying shocks on a daily basis when solving the model under alternative vaccination scenarios.

2.7 Solution

We solve our model in a similar way to Baqaee and Farhi (2024), where the higher-order terms are incorporated into the system via cross-factor and industry elasticities. By applying small perturbations to the system, and following the trajectory of the prices and wages, we arrive at a new equilibrium where the system re-optimizes around the old one. This methodology is akin to the Euler integration method to calculate the solutions of differential equations. Hence, we calculate differential exact hat-algebra to characterize the changes in the system by iterative means.

To compute the new equilibrium, we need to trace through the changes in prices and expenditure shares after we introduce pandemic-driven sectoral shocks. We trace the sectoral pandemic shocks to the supply term $-\Delta^{L}_{ic}(I_{c,t})$ in Equation (12)– and demand term $-\Delta^{0c}_{j}(I_{c,t})$ in Equation (13)– through inter-country input-output linkages. Any small perturbation to the system results in changes in the Domar weights and changes in prices. The relationship between changes in Domar weights and prices is governed by an exogenous labor shock,

allowing us to solve the model.

On the cost side, with Shepard Lemma, we can write all the price changes in terms of wage changes. Formally, we can write the changes in prices as (in matrix notation):

$$d\log p_{ic} = \sum_{jm \in \mathcal{CN}} \Omega^{ic}_{jm} d\log p_{jm} + \Omega^{\mathcal{F}}_{ic} d\log w_{ic} \Rightarrow d\log p' = \Omega^{\mathcal{N}} d\log p' + \Omega^{\mathcal{F}} d\log w'.$$

Solving for changes in prices in terms of changes in wages, we arrive at:

$$d\log p' = \Omega^{\mathcal{F}} \left(I - \Omega^{\mathcal{N}}\right)^{-1} d\log w' = \underbrace{\Omega^{\mathcal{F}} \Psi^{\mathcal{N}}}_{\equiv \Psi^{\mathcal{F}}} d\log w' = \Psi^{\mathcal{F}} d\log w'. \tag{14}$$

Focusing on the Domar weights of factors, we can also relate them to changes in prices and labor supply changes with:

$$d\Lambda_f = \Lambda_f d\log \Lambda_f = \Lambda_f (d\log w_f + d\log L_f) \Rightarrow d\log w = d\Lambda\, \hat{\Lambda}^{-1} - d\log L.$$

where $\hat{\Lambda}$ is the diagonal matrix whose diagonal elements are given by Λ. Hence, we can write the changes in log-wages in terms of changes in Factor Domar weights. Starting with Equation (9), we can write changes in the Domar weights as:[8]

$$d\Lambda = (d\chi\, \Omega^0 + \chi\, d\Omega^0 + \lambda\, d\Omega^{\mathcal{N}}) \Psi^{\mathcal{F}} + \lambda\, d\Omega^{\mathcal{F}}. \tag{15}$$

To solve the system, we will write all these terms in terms of $d\log \Lambda$ or equivalently $d\log w$. Note that the formulation is more general than the sector-specific labor case. If multiple factors are used, let's assume that these factors are combined with elasticity η. Consequently, we can pin down the changes in wages for any factor using the following proposition:

Proposition 1 *Given the supply shock* $d\log \Delta^L_{ic}$*, the sectoral demand shock* $d\log \Delta^{0c}_j$ *and the nested CES model explained in Sections 2.1 to 2.5, the changes in the wages satisfy:*

$$d\log w = d\log w\, A\, \hat{\Lambda}^{-1} + B\, \hat{\Lambda}^{-1} - d\log \Delta^L,$$

where $A = A_1 + A_{22} + A_{23} + A_{24} + A_{31} + A_{32} + A_{33} + A_{34} + A_{41} + A_{42} + A_{43}$*, and* $B = B_1 + B_{21}$ *such that:*

[8] The second equality comes from the fact that $d\Psi^{\mathcal{N}} = \Psi^{\mathcal{N}}\, d\Omega^{\mathcal{N}}\, \Psi^{\mathcal{N}}$ (dropping superscripts):

$$d(\Psi\, \Psi^{-1}) = 0 = d\Psi\, \Psi^{-1} + \Psi\, d\Psi^{-1} \Rightarrow d\Psi\, \Psi^{-1} = -\Psi\, d\Psi^{-1} \Rightarrow d\Psi = -\Psi\, d\Psi^{-1}\, \Psi = -\Psi\, d(I - \Omega)\, \Psi = \Psi\, d\Omega\, \Psi.$$

$$
\begin{aligned}
A_1 &= \hat{\Lambda}\,\Phi^E\,\Omega^0\,\Psi^{\mathcal{F}} & B_1 &= d\log\Delta^L\,\hat{\Lambda}\,\Phi^E\,\Omega^0\,\Psi^{\mathcal{F}}\\
A_{22} &= \Psi^{\mathcal{F}'}\,(1-\widehat{\xi^0})\,\widehat{\chi\Omega^0}\,\Psi^{\mathcal{F}} & A_{23} &= \Psi^{\mathcal{F}'}\,(\widehat{\xi^0}-\sigma)\,\left[(1_{C\times C}\otimes I_N)\odot\left(\Xi^{0'}\,\hat{\chi}\,\Omega^0\right)\right]\,\Psi^{\mathcal{F}}\\
A_{24} &= (\sigma-1)\,\Psi^{\mathcal{F}'}\,\Omega^{0'}\,\hat{\chi}\,\Omega^0\,\Psi^{\mathcal{F}} & B_{21} &= \sigma\,\chi\,(\Omega^0\odot d\log\Delta^0)\,\Psi^{\mathcal{F}}\\
A_{31} &= \Psi^{\mathcal{F}'}\,(1-\hat{\xi})\,\widehat{\lambda\Omega^{\mathcal{N}}}\,\Psi^{\mathcal{F}} & A_{32} &= \Psi^{\mathcal{F}'}\,(\hat{\xi}-\varepsilon)\,\left[(1_{C\times C}\otimes I_N)\odot\left(\Xi^{\mathcal{N}'}\,\hat{\lambda}\,\Omega^{\mathcal{N}}\right)\right]\,\Psi^{\mathcal{F}}\\
A_{33} &= (\varepsilon-\phi)\,\Psi^{\mathcal{F}'}\,\Omega^{\mathcal{N}'}\,\hat{\lambda}\,(1-\hat{\alpha})^{-1}\,\Omega^{\mathcal{N}}\,\Psi^{\mathcal{F}} & A_{34} &= (\phi-1)\,\Psi^{\mathcal{F}'}\,\hat{\lambda}\,\Omega^{\mathcal{N}}\,\Psi^{\mathcal{F}}\\
A_{41} &= (1-\eta)\widehat{\lambda\Omega^{\mathcal{F}}} & A_{42} &= (\eta-\phi)\,\Omega^{\mathcal{F}'}\,\hat{\lambda}\,\hat{\alpha}^{-1}\,\Omega^{\mathcal{F}}\\
A_{43} &= (\phi-1)\,\Psi^{\mathcal{F}'}\,\hat{\lambda}\,\Omega^{\mathcal{F}}. & &
\end{aligned}
\tag{16}
$$

Here, Δ^L represents the row-vector of labor supply shocks, Δ^0 represents $C\times CN$ matrix of sectoral demand shocks, $\odot$ ($\otimes$) represents Hadamard (Kronecker) product, $1_{C\times C}$ is the $C\times C$ matrix of ones, I_N is the identity matrix of size N, ξ and ξ^0 are the vector of sectoral elasticities matched to sector-industry combinations, hat ($\hat{}$) operator creates a diagonal matrix whose diagonal elements are given by the vector underneath it. To make the rank of A matrix full, we need to replace one equation with the fact that the total GDP of the world is not changing, i.e., $\sum_{f\in\mathcal{F}} d\Lambda_f = 0$. Hence:

$$A_{1,1} = 0, \quad A_{f>1,1} = -\Lambda_f$$

The proof of this proposition is provided in the online Appendix and requires careful differentiation at each step, combined with Shepard Lemma. The intuition behind each matrix is as follows:

- $\Psi^{\mathcal{F}}$ connects the good price changes to factor prices.
- A_1 matrix captures the direct income effect of a change in factor wage on spending. This is the linear Leontief inverse channel.
- B_1 vector captures the income effect of the labor declines.
- B_{21} vector captures the direct effect of sectoral demand shocks.
- A_{22} matrix captures the direct effect of price change in an industry due to shocks. The first and the last $\Psi^{\mathcal{F}}$ terms maps these changes to the factor prices.
- A_{23} matrix captures the substitution between factors due to differential substitutability of country varieties within sectoral consumption bundles. The $(1_{C\times C}\otimes I_N)$ term selects for varieties within the same sectors. Note that if all sector elasticities are the same as σ, this term would drop.

- A_{24} matrix captures the overall substitution between any two industries in consumption through the consumption price index.
- A_{31} is similar to A_{22}, but operates through input shares.
- A_{32} is similar to A_{23}, but operates through input sectoral bundles.
- A_{33} is similar to A_{24}, but operates through input bundles.
- A_{34} matrix captures the direct effect of price changes.
- A_{41} matrix captures the wage changes induced by the factor input channel. Note that When the factors are sector-specific and only a single factor is used in each sector, then $\widehat{\lambda \Omega^{\mathcal{F}}} = \widehat{\lambda \odot \alpha}$, where α is the vector of value-added shares.
- A_{42} matrix captures the factor substitution within the same industry. With sector-specific labor as the only factor $\Omega^{\mathcal{F}'} \hat{\lambda} \hat{\alpha}^{-1} \Omega^{\mathcal{F}} = \widehat{\lambda \Omega^{\mathcal{F}}} = \widehat{\lambda \odot \alpha}$. Hence, in this case, the contribution of $A_{41} + A_{42}$ becomes $(1-\phi)\widehat{\lambda \odot \alpha}$.
- A_{43} matrix captures the substitution between industries and factors. With the sector specific labor assumption, this term becomes $A_{43} = (\phi - 1)\, \Psi^{\mathcal{F}'} \hat{\lambda}\, \Omega^{\mathcal{F}} = (\phi - 1)\, \Psi^{\mathcal{F}'} \hat{\Lambda}$.

The normalization of world GNE / GDP, i.e., $E = 1$, only affects the prices to a multiplicative factor. Since we focus on real welfare changes, this multiplicative factor does not affect real output changes in sectors. As we do not compare prices between pre-Covid-19 and Covid-19 epochs, this normalization does not affect our results presented below. Hence, given the supply and demand shocks, $d \log w$ term can be solved with:

$$d \log w = B\, \hat{\Lambda}^{-1} (I - A\, \hat{\Lambda}^{-1})^{-1}.$$

where A and B are matrices summarizing all linear relationships in Equation (16).

From the changes in wages, we can calculate all other changes including Domar weights, prices, Input-Output (Ω) matrix, Leontief-inverse (Ψ) matrix, GDP, country-level expenditures, real GDP, and real expenditures. Briefly, from changes in factor prices and changes in labor supply changes, we can calculate changes in factor Domar weights. From the changes in factor Domar weights, we can calculate the changes in each country's income share, χ vector. On the other hand, using Shepard Lemma, we can easily find the changes in good prices. From changes in good prices and changes in factor prices, we can calculate the changes in consumption shares, input-output shares, and value-added share for each industry using the underlying elasticities in our nested production and consumption functions. Once we have these changes as well, we can calculate the changes in Domar weights

for goods using Equation (15). Given the price change and the Domar weight change, we can calculate the real production (GDP) change in each industry as:

$$d \log y_{ic} = d \log \lambda_{ic} - d \log p_{ic}.$$

Similarly, we can express the real expenditure (GNE) change of country c as:

$$d \log C_c = d \log \chi_c - d \log p_{0c}, \tag{17}$$

which is the nominal expenditure of country c divided by the consumption price index of country c, p_{0c}. Hence, the real "welfare" change linked to real expenditure change is endogenously determined.

As can be seen in Equations (5) and (13), underlying demand equations have different weight parameters during the shock period. Hence, to make post-pandemic real changes comparable with the pre-pandemic levels, we use a chained Törnqvist price index. This is a convenient tool to adapt for our framework because we chain small shocks to obtain a solution as in Baqaee and Farhi (2024). Our solution methodology approximates larger shocks by applying small shocks over many iterations. At each iteration, we recalibrate the model to ensure that all equations described in Sections 2.1, 2.2 and 2.3 reflect the new equilibrium. We provide the detailed calculations in Section F of the Online Appendix.

3 Data, Parameters and Variable Construction

3.1 Network and Employment

We utilize the OECD Inter-Country Input-Output (ICIO) Tables from 2015, covering 65 countries and 35 sectors, as depicted in Figure 1 in the introduction.[9] These tables detail the expenditure shares of each sector, illustrating the flow of funds to and from other sectors across countries, thereby capturing global input-output links (or sectoral exports/imports). We also use sectoral employment data from the OECD's Trade in Employment (TiM) database (Horvàt et al., 2020).[10]

[9] In the time of writing, 2015 table was the latest year for which the data was available. The OECD ICIO table aggregates 2-digit ISIC Rev 4 codes into 36 sectors. The last sector, "Private households with employed persons," lacks inter-industry linkages and is therefore excluded from our analysis, leaving us with 35 sectors. We refer to this classification as OECD ISIC Codes throughout our analysis.

[10] For 14 countries lacking data in the TiM database, we sourced employment data from the World Development Indicators database of the World Bank and allocate across sectors according to average shares in the countries where sectoral data is available.

To estimate the industry-level teleworkable share and physical proximity measures, we analyze the occupational composition of industries. We utilize the list by Dingel and Neiman (2020) to identify occupations capable of remote work. For employees who continue their roles on-site, we assume their infection risk is associated with the required physical proximity in their workplace. We derive these proximity requirements using the self-reported Physical Proximity values from the Work Context section of the O*NET database. O*NET categorizes physical proximity into five levels: (1) I don't work near other people (beyond 100 ft.); (2) I work with others but not closely (e.g., private office); (3) Slightly close (e.g., shared office); (4) Moderately close (at arm's length); (5) Very close (near touching). For analysis, we normalize these values by dividing them by 3, setting category (3) as our benchmark. Consequently, a proximity value greater than 1 signifies a closer interaction than 'shared office' level, and a value less than 1 indicates less dense working conditions. We calculate the proximity values after excluding the teleworkable segment of the workforce. A single proximity value for each occupation is then computed by weighting the normalized score according to the percentage distribution of responses across categories.

To determine the industry-level teleworkable share and proximity values, we calculate the weighted averages based on the occupations within each industry, utilizing the Occupational Employment Statistics (OES) from the U.S. Bureau of Labor Statistics (BLS). The OES data uses four-digit NAICS codes to classify industries. We then convert the proximity data to OECD ISIC codes using the correspondence table between 2018 NAICS and ISIC Revision 4 Industry Codes, provided by the U.S. Census Bureau. The teleworkable shares and proximity indices for each industry are displayed in Figure E.3 in the Appendix.

3.2 Elasticities of Substitution: Consumption, Production and Trade

Figure E.2 shows the nested CES structure of our model both on the production side and on the consumption side, combining Figures 2 and 3. For the closed economy, we use the same elasticities as in Baqaee and Farhi (2024). Producing "Good (Varieties)" requires combining labor and intermediate goods, which are complements. We set this elasticity to $\theta = 0.6$. The "intermediate bundle" captures the aggregation of alternative inputs such as steel and textiles, which are also complementary to each other. This elasticity is set to be $\varepsilon = 0.2$. This value is consistent with the estimates in the literature (Atalay, 2017) who find strong complementarities at this stage. On the consumption side, we set $\sigma = 1$ (Cobb–Douglas) as the elasticity of substitution between sectors, implying that a constant share of income is allocated across sectors according to their respective weights. We introduce our sectoral demand shocks through adjustments to these weights.

For an open economy, the "sector bundle" in our model allows for the substitution among input varieties from different countries, such as Turkish steel, Chinese steel, and U.S. steel, from the perspective of the U.S. industry. We apply industry-specific trade elasticities as measured by Caliendo and Parro (2015), where all varieties are considered substitutes. Additionally, we incorporate elasticity estimates from Boehm et al. (2019), which treat the input varieties as complements. This multilayer CES structure enables us to capture both substitution and complementarity—e.g., between Turkish steel and Canadian lumber imported by the U.S. construction industry, as well as between Turkish and Chinese steel for the same U.S. sector. On the consumption side, the structure also allows us to distinguish between the consumption of Turkish cars versus German cars by U.S. consumers.

3.3 Infection Dynamics

We employ the widely used Susceptible-Infected-Recovered (SIR) model, a fundamental workhorse in epidemiological studies.[11] Details of our implementation of the SIR model are provided in Section A of the Appendix. Our adaptation captures sectoral heterogeneity in infection rates by incorporating industry-specific proximity requirements and the potential for teleworkability within each sector.

Each of the 65 countries in our sample has a distinct experience regarding the course of the pandemic. In the SIR model, the two fundamental structural parameters, the resolution, and the infection rates, define the pandemic's trajectory. The resolution rate is a disease-specific structural parameter that does not vary much across the countries. According to the report by the WHO, the median recovery time for mild cases is approximately two weeks.[12] The mean recovery time could be longer when we include severe cases. In this paper, we err on the optimistic side and set recovery time, $\gamma = 1/14 \approx 0.07$ to establish a mean recovery time of 14 days. However, the infection rate might vary across countries depending on each country's success in containing it. Since the onset of the pandemic, the infection rate exhibits a varying pattern over time, which arises because of the various lockdown measures adopted by countries to reduce the transmission of the virus.

For the calibration of infection rate, β, we make use of publicly available data sets to trace this variation across countries and across time.[13] For each country, we estimate a SIR model described in Equations (A.1)-(A.3) using official data to reproduce the variation in

[11] See, for example, Allen (2017) among others.

[12] https://www.who.int/docs/default-source/coronaviruse/who-china-joint-mission-on-covid-19-final-report.pdf

[13] The data is downloaded from GitHub, Covid-19 Data Repository by the Center for Systems Science and Engineering (CSSE), at Johns Hopkins University.

the trajectory of pandemic across countries. To capture the variation within each country, we extend the SIR model to allow for time variation in the infection rate, i.e., β_t. We employ the methodology proposed in Çakmaklı and Şimşek (2024) to capture the changes in the rate of infection throughout the pandemic for the countries in our sample. This methodology involves estimating a SIR model with time-varying parameters in a statistically coherent way to accommodate various non-pharmaceutical interventions, including lockdowns.

Numerous studies employ the SIR model with fixed parameters to estimate the progression of infectious diseases (See, for example Hortaçsu et al., 2021). However, models that incorporate time-varying parameters are less common (e.g., Fernández-Villaverde and Jones, 2022, incorporates time variation in the infection rate). The time-varying parameters SIR model proposed by Çakmaklı and Şimşek (2024) offers two key advantages. First, it is statistically consistent with the count data structure typically associated with pandemic data, in contrast to models that rely on least-squares or likelihood-based inference assuming a normal distribution. Second, it achieves computational efficiency, which is essential given the extensive datasets involved, unlike models like the particle filter that are statistically robust but computationally intensive.

For our analysis, we use data from each country starting from the day the number of active infections exceeds 1000 until the end of December 2020. The parameter values, country-specific β_t, and γ are calculated as of the end of December 2020, reflecting the pandemic's status in each country at the time of the vaccine discovery. Using these values, we simulate the pandemic's progression in each country over the following year. To mitigate potential estimation errors due to parameter uncertainty, we typically imposed an R_0 between 1.1 and 1.3 for all countries, except for Australia, New Zealand, and China, which have been relatively successful in controlling infections. The R_0 values used are detailed in Table E.1.

Our model incorporates endogenous lockdowns triggered when the number of cases exceeds a threshold calibrated to the ICU capacity of each country. ICU capacity data is sourced from various entities including the WHO, the JHU data repository, and national health ministries. During a full lockdown, the infection rate drops to zero, effectively halting the spread of the virus. Each lockdown period lasts 14 days, during which the number of Covid-19 patients is reduced to 36% of its pre-lockdown level. After lifting the lockdown, we assume it takes 90 days for infection rates to return to the reproduction number observed prior to the lockdown.

Under a full lockdown, only essential industries remain operational. We identify which industries are closed during lockdowns based on international government decrees (detailed in Table E.3). Using disaggregated employment data, we calculate the share of each

OECD ISIC industry that remain active during a lockdown. Finally, we estimate the proportion of public employees unaffected by the lockdown using publicly available data.

3.4 Labor Supply Shocks

Extensive survey-based evidence from the U.S. indicates that Covid-19 was a major reason for workplace absences during 2021, as illustrated in Figure 5a. There is a strong correlation—0.84 —from July 2020 to July 2022 between Covid-19 cases and the number of people not attending work due to self-reported pandemic-related reasons, based on weekly data. Figure 5b further demonstrates that labor supply linked to health in the U.S. has not returned to pre-pandemic levels. The data reveal that the average number of individuals absent from work due to illness remains significantly higher during the pandemic than in the pre-pandemic period.

Figure 5: The Effects of Covid-19 on U.S. Labor Supply

(a) Not working due to Covid-19

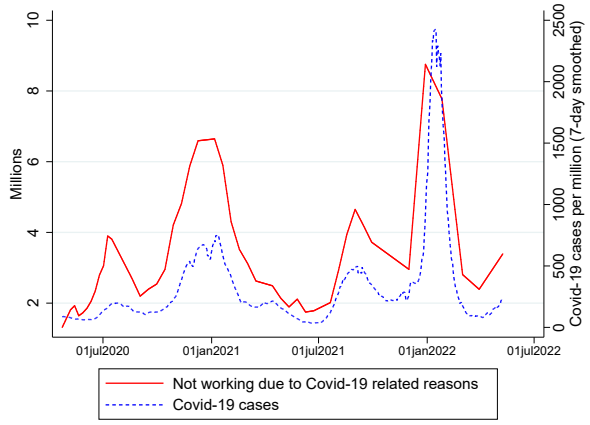

(b) Not working due to own illness over time

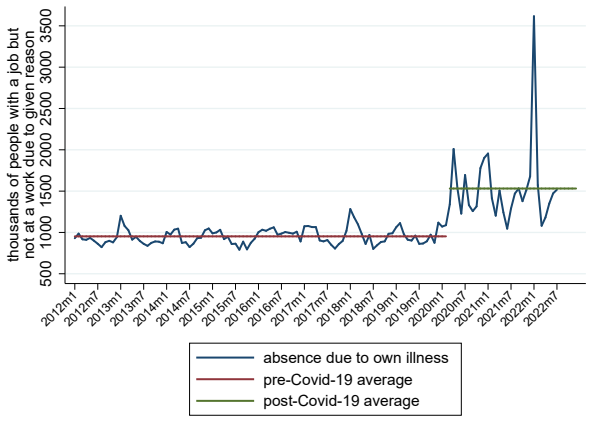

NOTES: Panel (a) displays the co-movement between the weekly number of individuals reporting an inability to work due to *pandemic-related reasons* and the weekly number of reported COVID-19 cases. For details on the construction of this data series, which is derived from the U.S. Census Bureau Household Pulse Survey, see Section B.1.

Panel (b) shows the monthly number of employed individuals in the U.S. labor market who were absent from work, spanning the period from January 2012 to July 2022. This series is based on the Current Population Survey conducted by the U.S. Bureau of Labor Statistics and captures monthly absences due to an individual's own illness, injury, or medical condition. For additional details, see Figure B.1 in Appendix B.2.

Sectors are heterogeneous in terms of the share of teleworkable jobs and physical proximity requirements, which results in differential sector-specific labor supply shocks during the pandemic. Once the virus hits and spreads among the workers, the total number of

workers in a given country-sector pair ic changes to $L_{ic,t}$ as a function of the infections and can be written as:

$$\Delta^{L}_{ic}(I_{c,t})\, L_{ic} = (N_{ic} - I_{ic,t}) + TW_{ic}\left(1 - \frac{I_{0c,t}}{N_{0c}}\right) = L_{ic} - I_{ic,t} - TW_{ic}\frac{I_{0c,t}}{N_{0c}} \tag{18}$$

where N_{ic} is the number of workers in the on-site group in industry-country pair ic, $I_{ic,t}$ is the number of infected workers in the on-site group, and TW_{ic} is the number of workers in the at-home group (i.e., those who can work remotely) in industry-country pair ic. We denote the vector of all infections in the country with $I_{c,t}$.[14] The ratio $I_{0c,t}/N_{0c}$ captures the fraction of infected individuals in the at-home group, which includes the non-working population as well as all workers in the at-home group (i.e., teleworkers). Figure 6a illustrates how our model generates labor supply shocks in response to pandemic dynamics. In Figure 6b, we present the model-implied labor supply shocks derived by feeding the actual number of COVID-19 infections in the United States into our framework. To distribute these country-level infections across sectors, we allocate them proportionally based on sectoral employment shares.

Figure 6: Labor Supply Shocks

(a) Labor during Pandemic

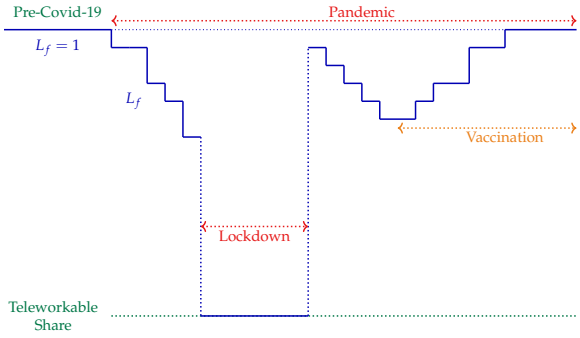

(b) Labor Supply Shock in the US vs Model

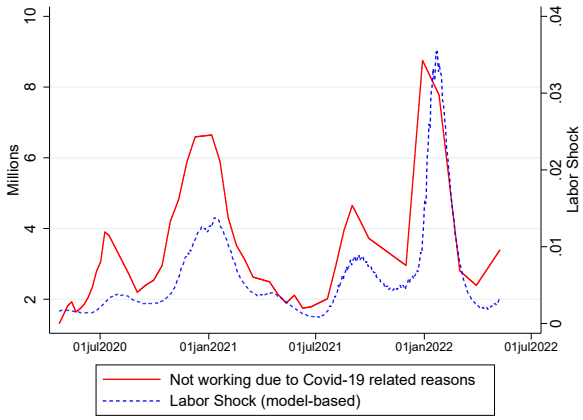

NOTES: Panel (a) illustrates the pattern of labor supply shocks during the pandemic. Panel (b) shows the co-movement between the weekly number of individuals reporting an inability to work due to *pandemic-related reasons* and the labor supply shocks for the U.S., as derived from our sectoral epidemiological model. The correlation between these two series is 0.82, highlighting the strong and direct impact of the pandemic's progression on labor supply. The data covers the period from April 23, 2020, to May 9, 2022. For details on the construction of this series, which is based on the U.S. Census Bureau Household Pulse Survey, see Section B.1.

[14] The ith element of $I_{c,t}$ corresponds to $I_{ic,t}$. With an abuse of notation, we start indexing the vector with 0.

Under lockdown conditions, only workers in non-essential industries who are able to telework can continue to work. In contrast, for essential industries, the number of available workers remains governed by the equation above.

Accordingly, the sector-specific labor shock for industry ic depends on three factors: the number of infected on-site workers, the share of teleworkable jobs in sector i, and the lockdown status in country c. The resulting sectoral labor supply shock can be expressed as:

$$\Delta_{ic}^{L}(I_{c,t}) = \begin{cases} \frac{L_{ic} - I_{ic,t} - TW_{ic}\frac{I_{0c,t}}{N_{0c}}}{L_{ic}} & \text{if } c \text{ is not under lockdown or } i \text{ is essential,} \\ \frac{TW_{ic} - TW_{ic}\frac{I_{0c,t}}{N_{0c}}}{L_{ic}} & \text{if } c \text{ is under lockdown and } i \text{ is non-essential.} \end{cases} \tag{19}$$

3.4.1 Reduced Form Evidence on Supply Shocks

Here, we provide two types of reduced-form evidence to validate the measurement of our shocks. First, we compare our model's infections-based sectoral supply shocks with actual data on workers who did not report to work due to pandemic-related reasons.[15] As detailed in Section B.1, 47 percent of U.S. households reported "pandemic-related" reasons for not working. Notably, the correlation between these two series is 0.82, underscoring the direct impact of the pandemic's progression on labor supply (Figure 6b in the Appendix).

As a second robustness check, we examine the co-movement between our labor shocks and real-time supply chain disruptions. To this end, we utilize the Suppliers' Delivery Time Index—a sub-index of the Purchasing Managers' Index (PMI)—and correlate it with our model-based labor shock. This labor shock is calculated by aggregating data across the manufacturing industries of 26 PMI-reporting countries, using trade shares as weights. We observed a high correlation of 0.78. Further evidence supporting this correlation, including additional data from surveys on labor and intermediate input shortages in the U.S. and Euro area countries, is presented in Appendix Section C.

[15] In June 2022, the Census Bureau enhanced the Household Pulse Survey by adding four questions about the current status and duration of Covid-19 symptoms, offering researchers improved insights into the prevalence of Covid-19 symptoms. A recent Brookings Report uses this data to estimate the impact of long Covid on the U.S. labor market. As of August 2022, it is estimated that 16 million working-age Americans (aged 18 to 65) suffer from long Covid, with 2 to 4 million unable to work because of their condition. For more details, please visit https://www.brookings.edu/research/new-data-shows-long-covid-is-keeping-as-many-as-4-million-people-out-of-work/.

3.5 Consumption and Sectoral Demand Shocks

The OECD ICIO Tables provide input demand data for industry i in country c from any industry in any country. The final demand vector comprises 2340 entries indexed by ic, corresponding to country-industry combinations. By dividing the rows of the ICIO matrix by the total output of industry ic, we obtain the direct requirements matrix Ω. This matrix summarizes the usage of each intermediate input to generate \$1 worth of output. The output of each industry is either used as an intermediate input or consumed as final output.

For the changes in the composition of consumption, specifically the sector-specific demand shifter $\Delta_j^{0c}(I_{c,t})$ in equation (13), we use U.S. sectoral personal consumption data and predict the changes as a function of infections. Because we use a Cobb–Douglas consumption aggregator with $\sigma = 1$, changes in the observed expenditure shares directly reveal the demand weight shocks. We use the monthly data, sourced from the Bureau of Economic Analysis, from February 2020 to the end of 2020 (Figure 7a). Corresponding data for other countries is unavailable. Therefore, we first perform a non-parametric regression of U.S. sectoral personal consumption on U.S. sectoral infections using a second-order polynomial. From these estimates, we calculate the sector-specific consumption changes for other country-sectors based on their respective sectoral infections.[16]

We conducted two robustness checks on the estimated sectoral consumption data for the remaining countries, with the results presented in the Appendix. First, we report the R^2 values to assess whether infection rates explain a greater share of consumption variation in services sectors. This pattern is indeed confirmed, as illustrated in Figure 7b. Second, for Turkey—where detailed credit card spending data by sector is available—we compare our infection-based estimates of sectoral consumption changes with those derived from actual credit card spending. The comparison reveals a strong correlation between the two measures, as shown in Figure 7c.

4 Quantitative Results

4.1 Vaccination Scenarios

In our empirical exercises, we first assume a vaccination scenario, which determines the sectoral shocks we input into the model. Under full vaccination, there are no sectoral shocks.

[16] We perform several robustness checks to address the sensitivity of non-parametric estimation to functional forms and extreme values in infections data, including higher-order polynomials to capture any remaining nonlinear patterns in the consumption-infection relationship.

For any other scenario, sectoral shocks are present. Vaccination patterns influence the progression of the pandemic in our SIR model by directly moving susceptible individuals into the recovered group. Since both our sectoral labor shocks (Equations 18 and 19) and the sectoral demand shifters ($\Delta^{0c}j(Ic,t)$, as described in Section 3.5) depend on the number of individuals in the infected group, different vaccination scenarios lead to different shock magnitudes.

Figure 7: Demand Shocks

(a) Sectoral Demand in the U.S.

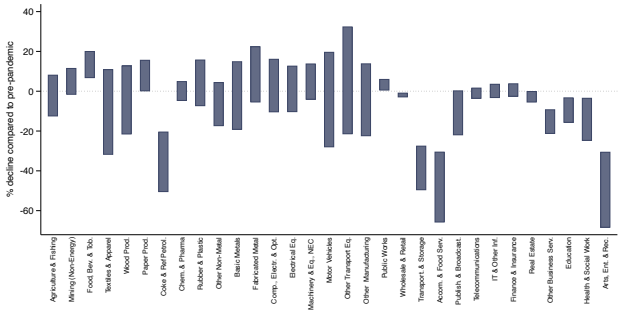

(b) Goodness-of-Fit

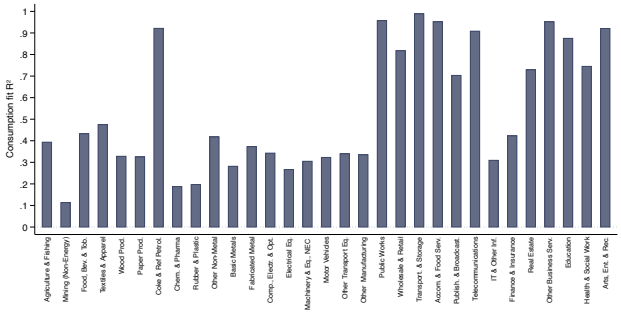

(c) Sectoral Demand— Credit Card Data

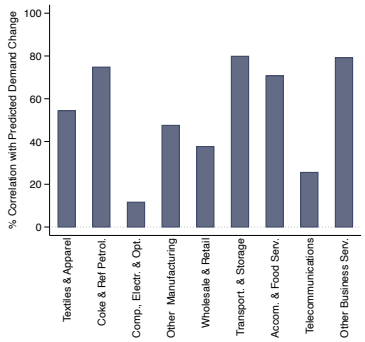

NOTES: Panel (a) presents the range of changes in sectoral personal consumption data for the U.S., showing the minimum and maximum observed values. The data are at monthly frequency and sourced from the Bureau of Economic Analysis (BEA) for the period from March 2020 through the end of 2021. Following Baqaee and Farhi (2022), we compute monthly changes in consumption relative to February 2020. To estimate demand changes, we first run sector-level regressions, fitting consumption declines to a second-degree polynomial in the number of infections. Panel (b) reports the goodness-of-fit for each sector using R^2 values. Sectors such as Mining and extraction of energy-producing products, Mining support service activities, Construction, and Public administration and defense; compulsory social security show no variation in the reported data and are therefore omitted for clarity. Panel (c) displays the correlation between predicted and actual demand changes by sector in Turkey, covering the period from week 11 to week 26 of 2020 (corresponding to the first three months after the initial COVID-19 case was reported in the country). Predicted demand changes are estimated using the methodology described in Section 3.5. Weekly changes in credit card spending are calculated relative to the four-week average from week 7 to week 10 of 2020. Based on the mapping between CBRT industry codes and OECD ISIC industries, we exclude sectors in which credit cards are not commonly used as a payment method, thereby limiting the coverage to relevant sectors.

After inputting the sectoral shocks, we calculate the relative reduction in welfare for each country using Equation (17), as detailed in Section 2.7. To aggregate country-level losses to the country-group level (i.e., AEs vs. EMDEs), we weight each country's change by its 2019 GDP.

Our alternative vaccination scenarios are summarized in Table 1.[17] Scenario I is a counterfactual where AEs are vaccinated immediately upon vaccine discovery, corresponding to the start of the model's second period, while EMDEs do not receive vaccinations. The two sub-scenarios that are related to the first scenario are vaccine transfer scenarios I-A and I-B which allow for immediate vaccination of AEs (100% of AE population in I-A and 80% in I-B) and transfer of vaccines from AEs to EMDEs. The last scenario (Scenario II) is meant to mimic the actual vaccine rollout, where AEs are vaccinated faster than EMDEs throughout the second period. AEs complete their vaccinations midway through the period, whereas EMDEs, despite ongoing vaccinations, do not fully inoculate their populations by the end of the period. This scenario closely mirrors real-world conditions as of the end of 2021.

How do we map our two-period model to the rich dynamics of the second period? Our first period represents the pre-pandemic phase. We divide the second, pandemic period into 365 days to capture the heterogeneity during 2021, solving the model daily with daily sectoral supply and demand shocks. Due to the rapid vaccination rollout in the AEs, we stop incorporating shocks by the 120th day. This is consistent with reality, since by mid-2021, the average number of infections in the AEs had declined to low levels.

Table 1: Vaccination Scenarios

Scenario	AEs	EMDEs
I	Immediate Complete Vaccination	No Vaccination
I-A	Immediate Complete Vaccination	50% from AEs
I-B	Immediate 80% Vaccination	50+20% from AEs
II	Fast Vaccination	Slow Vaccination

4.1.1 Scenario I: Immediate Vaccination in AEs and No Vaccination in EMDEs

With this counterfactual scenario, our goal is to illustrate the costs incurred by fully vaccinated AEs solely due to their trade connections with the unvaccinated world, even though they completely eliminate the pandemic domestically. Therefore, there are no sectoral de-

[17] We assume that vaccination proceeds at the same pace across different segments of society.

mand and supply shocks in the AEs. In EMDEs, the pandemic evolves without access to any vaccine and can only be contained by lockdowns. Countries impose lockdowns when the number of Covid-19 patients requiring ICUs exceeds the number of ICUs reserved for Covid-19 patients.

Table 2: Model-Implied Real Expenditure Losses Relative to the Pre-Pandemic Levels under Scenario I (percent)

		Scenario I			
Consumption & Production Trade Elasticities		**World**	**Share of AEs (%)**	**AE**	**EMDE**
(1)	ξ_i^0, ξ_i =0.50	1.641	43.0	1.243	2.164
(2)	ξ_i^0, ξ_i =0.60	0.866	29.6	0.451	1.411
(3)	ξ_i^0, ξ_i =0.70	0.740	22.7	0.296	1.322
(4)	ξ_i^0, ξ_i =0.80	0.688	18.2	0.221	1.302
(5)	ξ_i^0, ξ_i =0.90	0.661	15.0	0.175	1.299

NOTES: This table presents the real expenditure losses under Scenario I. In this counterfactual scenario, we assume that the pandemic is fully contained in AEs immediately, while in EMDEs, the pandemic evolves naturally. We assume endogenous lockdowns in EMDEs when the number of Covid-19 patients requiring ICUs exceeds the number of ICUs reserved for Covid-19 patients. Consumption and production trade elasticities, ξ and ξ^0, have the same value in each row, and we increase both to capture the effect of higher substitution from row (1) to row (5).

We present the estimated real output losses for the world and by country groups in Table 2 relative to their pre-pandemic levels. In this table, the second column presents the total global loss in terms of pre-pandemic World GDP. The third column illustrates the relative cost of AEs as a fraction of the total global cost. The fourth and fifth columns break down this total cost into those incurred by AEs and EMDEs, respectively, which are expressed as a percentage of their own pre-pandemic expenditure levels. We set both the consumption and production trade elasticities to the same value and increase them together from row (1) to row (5). Focusing on row (1), we observe that the total world real output loss can be as high as 1.9 percent of pre-pandemic GDP. This first row represents an extreme case where the trade elasticities are set at 0.5. As the trade elasticities increase and countries can substitute goods and inputs imported from different countries, the overall costs decrease for everyone. The costs incurred by EMDEs are significantly higher compared to AEs because EMDEs are not vaccinated under this scenario. The share of the world output loss borne by the AEs decrease steadily from 26 percent to 7 percent as the elasticity of substitution increases. Evidently, when there are no domestic sectoral shocks, the losses from

international linkages are smaller for AEs as the elasticity of substitution is higher. Under the empirically-relevant elasticity of 0.6 in the short-run, the global loss is almost 1% of pre-pandemic GDP, with AEs shouldering 15 percent of this loss.

Figure 8: Model-Implied Real Expenditure Losses under Scenario I (percent)

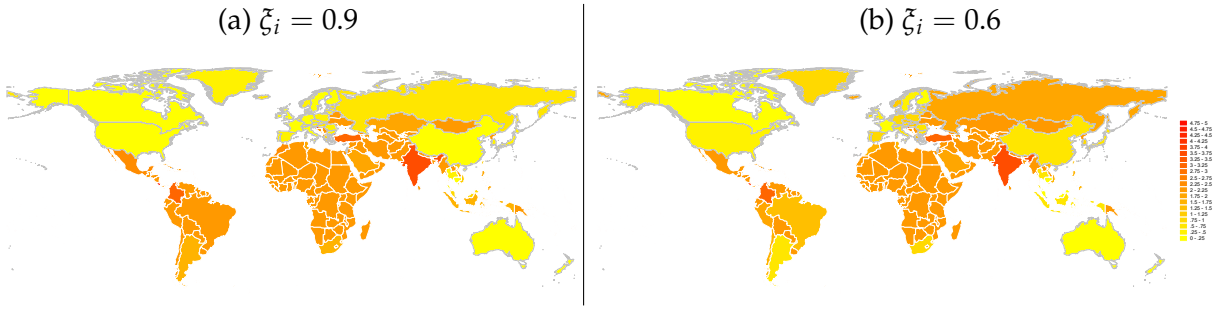

NOTES: This figure shows the reductions in real expenditure under Scenario I for two alternative trade elasticities in Panels (a) and (b), respectively. Vaccinated countries are distinguished by light gray borders.

Figure 8 displays the last two columns of the table visually so that the reader can see the country heterogeneity in terms of reductions in countries' real expenditure for 2021, relative to 2019, in percentage terms. Darker shades illustrate higher loss, and vaccinated countries are denoted by gray borders. We report two sets of estimates for comparison. High trade elasticity (left panel) corresponds to values reported in row (5) of Table 2, while low trade elasticity (right panel) corresponds to row (2) in the same table. At first glance, the lighter shades of the vaccinated countries are immediately noticeable in both panels. As we move from high trade elasticity to relatively low trade elasticity, the relative reduction in real welfare increases, indicated by the darker shades. This is consistent with the intuition that lower trade elasticity reflects the difficulty in substituting among suppliers, leading to more expensive and limited imports of intermediate inputs.

Table 3 considers two additional counterfactual scenarios and compare them to scenario I. In scenario I-A, we assume that AEs possess only the needed dosage of vaccines sufficient for their population. At the onset of 2021, developed countries were securing vaccine contracts in quantities well above their population needs. Scenario I-A considers the counterfactual case of AEs only keeping vaccines for their populations and send the excess vaccines to EMDEs. We assume this surplus amounts to 50% of the AEs' population. This additional supply accelerates and improves the reach of vaccination in EMDEs such that one-thirds of the EMDE population gets vaccinated within eighth months. This assumption is consistent with the results in Ledford (2022) who show that low and middle income nations would suffer less losses if they got the vaccines earlier.

In scenario I-B, we consider the case where developed countries procure vaccines sufficient for only 80% of their population and send the equivalent of 20% of their population's vaccine doses to EMDEs in addition to the surplus considered in Scenario I-A. This counterfactual case also never happened but considered by few countries such as France. In both scenarios, the model settings, including trade elasticities, are identical to those in Scenario I. We present here only two cases, elasticities set to $\xi_i^0 = \xi_i = 0.5$ and $\xi_i^0 = \xi_i = 0.6$, for illustration as provided in Table 3.

Table 3: Model-Implied Real Expenditure Losses Relative to the Pre-Pandemic Levels (percent): The Role of Vaccine Transfers

	Vaccination Scenario	Consumption & Production Trade Elasticities	World	Share of AEs (%)	AE	EMDE
(1)	Scenario I	$\xi_i^0, \xi_i = 0.50$	1.641	43.0	1.243	2.164
(2)	Scenario I-A	$\xi_i^0, \xi_i = 0.50$	0.837	47.8	0.705	1.010
(3)	Scenario I-B	$\xi_i^0, \xi_i = 0.50$	0.703	40.1	0.496	0.974
(4)	Scenario I	$\xi_i^0, \xi_i = 0.60$	0.866	29.6	0.451	1.411
(5)	Scenario I-A	$\xi_i^0, \xi_i = 0.60$	0.433	31.7	0.241	0.684
(6)	Scenario I-B	$\xi_i^0, \xi_i = 0.60$	0.462	39.6	0.323	0.646

NOTES: This table presents model-implied country-level real expenditure losses under two scenarios that are computed to understand the resulting economic losses/gains if advanced economies (AEs) delivered a part of their vaccines reserved for their population to emerging markets and developing economies (EMDEs).

Under empirically-relevant elasticities in the short-run, Scenario I-A demonstrates that total costs in the world economy decrease substantially to 0.44% of pre-pandemic world income, compared to 0.86% in Scenario I, where EMDEs are not vaccinated. In Scenario I-A, partial vaccination of EMDEs reaches one-third of the population within eight months. This results in a sharp decline in AEs' losses to 0.07% of pre-pandemic AEs' GNE, a significant reduction of over 70% compared to the case where no EMDEs are vaccinated (0.23%). The implication is clear: if EMDEs were at least partially vaccinated at no cost to AEs, as in Scenario I-A, AEs would benefit due to their trade and production linkages with EMDEs. Our message is straightforward: vaccinating poor countries mitigates the economic impact on rich countries through these linkages.

In Scenario I-B, the losses incurred by AEs are higher since now only 80% of the AE population is vaccinated. The world loss still goes down, though now AEs own costs and their share of global loss are both increased. Still, these results highlight the significant gains from trade and production linkages due to the improved ability of EMDEs to manage the pandemic with the additional vaccines provided by AEs.

4.1.2 Scenario II: Fast Vaccination in AEs and Slow Vaccination in EMDEs

This scenario aims to resemble the actual vaccination roll-out in real life. AEs are not fully vaccinated immediately, while EMDEs have access to the vaccine at a slower rate. AEs start vaccination early, with half of the susceptible population getting vaccinated in the first 30 days and the remaining half within the following 90 days. Thus, we assume that the vaccination of all susceptible populations in AEs will be accomplished within 120 days.

In contrast, EMDEs are unable to fully inoculate their susceptible populations due to a lack of sufficient vaccines, as was the case in 2021. Their vaccination program starts simultaneously with the AEs but takes a full year to vaccinate half of the susceptible population.

Table 4 shows the results. We observe the highest cost in row (1), with the total world real output loss at 1.5 percent of pre-pandemic GDP. We set the two trade elasticities to 0.60 in row (2), which serves as our baseline for the rest of the exercises. In our baseline case, the global output loss is approximately 0.8 percent. As the trade elasticities increase, it becomes easier to substitute varieties from different countries, thereby lowering the output losses. As the trade elasticities increase, the relative costs of AEs approach half of the total global costs, even though they are vaccinated faster.

Table 4: Model-Implied Real Expenditure Losses Relative to the Pre-Pandemic Levels under Scenario II (percent)

		Scenario II			
	Consumption & Production Trade Elasticities	**World**	**Share of AEs (%)**	**AE**	**EMDE**
(1)	ξ_i^0, ξ_i =0.50	0.979	40.8	0.703	1.341
(2)	ξ_i^0, ξ_i =0.60 (Baseline)	0.671	45.2	0.534	0.852
(3)	ξ_i^0, ξ_i =0.70	0.610	47.5	0.511	0.741
(4)	ξ_i^0, ξ_i =0.80	0.586	48.6	0.502	0.697
(5)	ξ_i^0, ξ_i =0.90	0.574	49.2	0.497	0.674
(6)	Caliendo and Parro (2015)	0.539	51.1	0.485	0.610

NOTES: This table presents the model-implied real expenditure losses under Scenario II. AEs follow a vaccination calendar to vaccinate the full population within four months, whereas EMDEs follow a more gradual vaccination calendar, with only half of the population getting vaccinated in one year. Production and consumption trade elasticities, ξ and ξ^0, have the same value in each row, and we increase both to capture the effect of higher substitution from row (1) to row (5). In the last row, we set those to the values computed by Caliendo and Parro (2015); these values are generally greater than 4, implying a high degree of substitution.

Evidently, when both AEs and EMDEs deal with their own domestic shocks, a higher

degree of substitution decreases the losses of EMDEs more than the AEs such that the share of AEs in total cost increases. What is the underlying intuition for this finding? According to our model, the economic costs that arise from supply chain disruptions are inversely related to: (i) *The variance in expenditure shares across origins:* Ceteris paribus, if one supplier is suffering from the pandemic, as long as a large share of expenditure is not concentrated in that supplier, the presence of alternative trade partners allows the importer to switch to another supplier and diversify its expenditures across origins. (ii) *The exposure of the suppliers to the health shock:* If a country has more suppliers that are vaccinated, then this country would be subjected to fewer disruptions in its supply chains.

What does the data tell us? As shown in Figure 1, the EMDEs are relatively more closed economies compared to AEs. This means that EMDEs operate with fewer suppliers to begin with. Additionally, AEs tend to trade more with other AEs. Given that EMDEs already have fewer suppliers and a larger fraction of these suppliers are unvaccinated (compared to AEs), potential disruptions in major suppliers are more likely for EMDEs. Consequently, these disruptions hit EMDEs harder because they have limited options for alternative suppliers. The story is different among AEs. The exposure of AEs to a specific supplier is already less, thanks to their more diversified integration into the international trade network. In a way, they do not put all their eggs in one basket. Furthermore, because a larger fraction of their trade partners are vaccinated, they are exposed to fewer health shocks. Thus, at any given level of elasticity of substitution, AEs not only have a lower likelihood of health shock exposure but also can diversify (and hence reduce) the size of the health shock. This helps them mitigate the economic costs of the pandemic.

As we increase the elasticity of substitution, EMDEs gain greater flexibility to switch to alternative suppliers during major disruptions, which significantly lowers their costs. For AEs, the cost reduction from increased elasticity of substitution is less pronounced because their diversified supplier base already mitigates reliance on any single supplier. Additionally, because AEs have more vaccinated trade partners, their need for substitution (and the consequent benefits from it) is relatively lower.

Consequently, the share of AEs' costs in world welfare loss increases with higher elasticities while EMDEs' losses decrease. This crucial finding emphasizes the interplay between international linkages and domestic shocks. On-shoring the supply chains may not be a panacea and could even be counterproductive. This result suggests that maintaining a level of global diversification in supply chains can be advantageous, especially for EMDEs, by providing the necessary flexibility to effectively mitigate disruptions.

Row (6) of Table 4 presents the results for the trade elasticity values estimated by Caliendo

and Parro (2015). These values can be interpreted as long-run elasticities with a higher degree of substitution. The results are consistent with the rest of Table 4. As the elasticities of substitution increase further, the share of AEs in world welfare losses approach 50 %. This outcome is attributed to the same compositional effect, where a high degree of substitution benefits EMDEs more significantly.[18]

Figure 9 displays the relative reduction in countries' real expenditure under Scenario II in percentage terms, for both low and high trade elasticities. The colors in both panels are darker for AEs, reflecting higher costs. Compared to Scenario I, AEs face additional factors that work in opposite directions. On the one hand, their vaccination calendar is now slower, which increases their domestic losses. On the other hand, their EMDE trade partners now have access to the vaccine, which reduces the losses from international linkages.

Figure 9: Model-Implied Real Expenditure Losses Relative to the Pre-Pandemic Levels under Scenario II (percent)

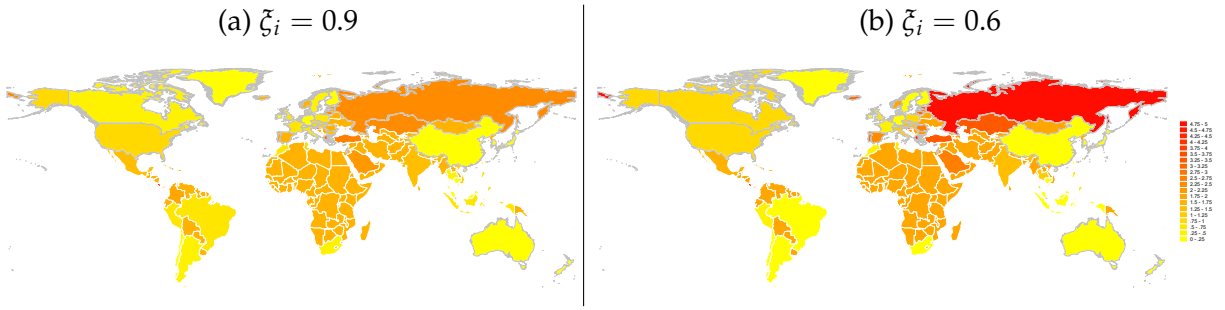

NOTES: This figure displays the reductions in real expenditures under Scenario II, with results shown for two alternative trade elasticity values in Panels (a) and (b), respectively. Countries with access to vaccines are outlined in light gray for visual emphasis.

Comparing Figure 8 and Figure 9, AEs' slower pace of domestic vaccinations outweigh the trade partners' access to the vaccine, yielding a net negative impact for AEs as we move from Scenario I to Scenario II. This is an important result that shows the right path for equitable global vaccinations: not to share limited supplies of AEs, since then domestic pandemic will stay, but rather invest in global production of vaccines.

Turning to the EMDEs, the sharp reduction in costs borne by EMDEs is immediately noticeable with the lighter shades. This is because EMDEs also have access to the vaccine in this scenario. The darker shade for Russia is interesting. Russia is a major exporter to AEs.

[18]There are endogenous lockdowns in both sets of countries here. We also consider another counterfactual scenario where we do not allow for any lockdown measures. The results for this scenario are presented in Table E.4 in the Appendix.

Hence, when the AEs are subject to a slower pace of vaccinations, the Russian economy is also adversely affected by lower demand in AEs for their exports.

4.2 Robustness: Counterfactual Shocks and Linkages

We consider two counterfactuals. In the first, we assume there is no international production network (no IPN). In the second, we assume that there are no relative demand shocks to change the composition of consumption across sectors. The only shocks present are to labor supply.

Table 5: Model-Implied Real Expenditure Losses Relative to the Pre-Pandemic Levels under Scenario II (percent): The Role of International Linkages and Demand Shocks

	Scenario II			
	World	**Share of AEs (%)**	**AE**	**EMDE**
Baseline	0.671	45.2	0.534	0.852
(1) No IPN	0.565	52.2	0.519	0.625
(2) No DS	0.683	52.0	0.625	0.759

NOTES: This table reports country-level real expenditure losses under Scenario II. "No IPN" refers to the case without International Production Networks, while "No DS" denotes the absence of sectoral demand shocks. The Baseline scenario assumes both consumption and production trade elasticities of $\xi_i^0 = 0.6$ and $\xi_i = 0.6$, respectively. The "No DS" case uses the same elasticity values, whereas the "No IPN" scenario reflects an autarkic setting in which countries are closed to international trade.

Table 5 displays the results for these two counterfactuals. We report the baseline findings for Scenario II for comparison purposes (top row). Row (1) shows the first counterfactual case of no international production network (no IPN). In this analysis, there are no international I-O linkages, so there is no trade for consumption and production inputs (or final goods); only domestic I-O linkages exist. The share of AEs' costs increased to 56.7 %. The costs increase we shut down the amplification role of the global network because production in AEs relies heavily on the network.

Row (2) of Table 5 shows the results from the second counterfactual of no demand shocks (no DS). We observe that, in the absence of demand shocks, there is a decline in real output loss for AEs compared to the baseline. This is an interesting result. By keeping the supply shocks the same and only removing the demand shocks, we obtain lower output losses. This indicates that relative sectoral demand shocks amplify the negative effects of sectoral supply shocks for the AEs.

The intuition for this result comes from the segmented labor markets. Sectors facing higher demand cannot attract more labor from other sectors; however, they do take inputs from other sectors. Due to diminishing returns on the inputs, this results in a loss in real output. This finding is independent of complementarities. An example based on a two-sector stylized economy is provided in Appendix Section D.

4.3 Robustness: Asymmetric Consumption and Production Trade Elasticities with Domestic Complementarities

In rows (1) to (3) of Table 6, we display robustness results where we increase the elasticity of substitution on the production side for traded inputs as before, but we leave the trade elasticity of the consumption of final goods, ξ_i', constant, exceeding 1. Intuitively, this exercise depicts an environment where a consumer can switch from an imported car to a domestic car under shocks. However, on the production side, if domestic car production needs foreign parts, there can be varying degrees of substitution for these parts. We obtain the same qualitative result as before: a higher degree of substitution in intermediate inputs helps EMDEs more than AEs. The share of AEs' costs increase as we move from rows (1) to (3), regardless of the ease of substitution for final consumption goods.

Table 6: Model-Implied Real Expenditure Losses Relative to the Pre-Pandemic Levels under Scenario II (percent): The Role of Production Elasticities

		Scenario II			
Consumption & Production Trade Elasticities		**World**	**Share of AEs (%)**	**AE**	**EMDE**
Baseline	$\xi_i' = 0.6, \xi_i = 0.6$	0.671	45.2	0.534	0.852
(1)	$\xi_i' = 1.1, \xi_i = 0.5$	0.607	46.5	0.497	0.750
(2)	$\xi_i' = 1.1, \xi_i = 0.6$	0.590	47.7	0.496	0.714
(3)	$\xi_i' = 1.1, \xi_i = 0.9$	0.568	49.3	0.493	0.665

NOTES: This table presents the model-implied country-level real expenditure losses under Scenario II. We vary ξ, the trade elasticity for the production side, but keep ξ^0, the trade elasticity for the consumption side, constant.

Next, we examine robustness for complementarities within countries. Table 7, rows (1) and (2), changes the value of σ, which controls the elasticity of consumption between different domestic sectors. The baseline uses $\sigma = 1$. With higher σ, output losses decrease for EMDEs. Interestingly, when σ is lower, the losses for EMDEs increase. We do not have a solid intuition for this result, but we suspect it is due to the interaction between more severe lockdowns in EMDEs, during which difficulty in consumption substitution across sectors

can have more negative effects. In row (3), we change the value of θ, which controls the substitution between labor and the intermediate bundle. When we increase the elasticity from 0.6 to 1.5, the costs decline for everyone, as the negative labor supply shock is more easily substituted by intermediate inputs.

Table 7: Model-Implied Real Expenditure Losses Relative to the Pre-Pandemic Levels under Scenario II (percent): The Role of Production and Consumption Elasticities

		Scenario II			
	Elasticities	World	Share of AEs	AE	EMDE
Baseline	$\xi_i^0 = 0.6, \xi_i = 0.6$	0.671	45.2	0.534	0.852
(1)	ξ_i^0, ξ_i =0.60, σ =1.5	0.645	43.6	0.495	0.842
(2)	ξ_i^0, ξ_i =0.60, σ =0.5	0.738	47.8	0.621	0.893
(3)	ξ_i^0, ξ_i =0.60, θ =1.5	0.619	52.4	0.571	0.682
(4)	ξ_i^0, ξ_i =0.60, ε =0.5	0.645	47.9	0.544	0.779
(5)	ξ_i^0, ξ_i =0.60, ε =1.5	0.615	51.1	0.553	0.695
(6)	Cobb-Douglas	0.560	52.9	0.521	0.610

NOTES: This table presents the model-implied real expenditure losses under Scenario II. Each row corresponds to a different elasticity specification. The row labeled "Cobb-Douglas" refers to the case where all trade and production elasticities are set to 1, reflecting unitary elasticity across all sectors.

In rows (4) and (5) of Table 7, we increase ε, the elasticity of substitution between sector bundles forming the intermediate bundle, from 0.2 to 0.5 (row (4)) and later to 1.5 (row (5)). The costs decrease with higher substitutability, but the share of AEs in world welfare losses increases. In rows (6), we show the results for Cobb-Douglas, for both consumption and production trade elasticities.[19] Both AE and EMDE losses are much lower under Cobb-Douglas, with a much higher degree of substitution under Cobb-Douglas. However, the share of the world welfare losses borne by AEs is higher under Cobb-Douglas, again as substitutability helps EMDEs more.

4.4 Evaluating Model's Fit in the Cross-Section

The pandemic affected different sectors of the economy and various countries in uneven ways. These heterogeneous effects can be observed through several data sources. For example, the European Commission's Business and Consumer Survey (EC-BCS) directly asks firms in different sectors about the main factors limiting their production. Meanwhile, the Industrial Production Index (Eurostat-IP) captures actual production levels across sectors.

[19] $\sigma = 1$, $\theta = 0.6$, and $\varepsilon = 0.2$ here as in the baseline.

To measure nominal output, we rely on data from Orbis. The empirical evidence presented in Appendix C highlights the sectoral and cross-country disparities in the impact of the pandemic. In this section, we compare the outcomes from our realistic scenario (Scenario II) with observed changes in the real world, using the data sources described in Appendix B.3.

We begin by comparing the actual changes in country-level GDPs with the predictions from our model. Our open-economy framework measures deviations from the steady state in terms of domestic absorption and expenditures (GNE). To approximate the pre-pandemic steady state, we use GDP growth rates from 2011 to 2019 at the country level, as these closely reflect the growth of GNE. We project this trend forward to 2021 to construct a counterfactual scenario without a pandemic. The difference between this projected growth and the actual growth observed during 2020–2021 gives us the realized deviation. We then compute the model-implied growth for the same period using Scenario II, which assumes that AEs achieve full vaccination and recover, while EMDEs do not recover due to limited access to vaccines. It is important to note that countries implemented extraordinary fiscal and health measures to cushion the economic impact of the pandemic. Moreover, many EMDEs ultimately gained access to vaccines, contrary to initial expectations at the beginning of 2021. For these reasons, our model is not intended to replicate the exact levels of growth but rather to capture the cross-country ranking where EMDEs fared relatively worse than AEs. Figure E.4 compares model-implied growth rates with observed deviations from trend growth. The correlation between the two is 23%. The main outliers—Philippines, Malaysia, and Cambodia—experienced a sharper incidence of the pandemic in 2021 than in 2020. Because our pandemic parameters are calibrated using 2020 data, with the initial infection level set to the realized cases at the end of 2020, the model underestimates the contraction in these economies. Excluding these countries increases the correlation to 39%, and for advanced economies only, the correlation rises further to 63%.

Combining data on sectoral input shortages with sectoral output and prices, we test: (i) the relationship between actual input shortages and actual sectoral output, (ii) the relationship between model-implied sectoral output changes and actual output changes, (iii) the relationship between actual input shortages and model-implied price changes, (iv) the relationship between model-implied sectoral price changes and actual price changes.

Table 8: EVALUATING MODEL FIT - I

Sample: Dep Var: %ΔY (Data)	**Eurostat-IP** Real Output (1)	**Eurostat-IP** Real Output (2)	**BvD-Orbis** Nominal Output (3)	**OECD-NAS** Nominal VA (4)
Input Shortage (from **EC-BCS**)	-0.9662** (0.350)			
% Δ Real Output (Model)		0.4323** (0.182)		
% Δ Nominal Output (Model)			0.1731** (0.058)	
% Δ Nominal VA (Model)				0.2061*** (0.051)
No. of Countries	21	21	27	42
No. of Sectors	16	16	35	7
Country FE	yes	yes	yes	yes
Obs.	282	282	928	290
R^2	0.25	0.35	0.48	0.13

NOTES:

In column (1), we regress sectoral industrial production changes on sectoral input shortages during the pandemic. In column (2), we use the same left-hand-side variable as in column (1) and regress it on the sectoral real output changes predicted by our model. For these two columns, actual output growth rates are calculated using 2-digit NACE Rev. 2 codes and aggregated to 2-digit OECD ISIC Rev. 4 codes using sector-level industrial production data from Eurostat. In column (3), we use gross nominal output (firm revenue) from firm-level balance sheet data in BvD-Orbis, aggregate to the sector level, and regress the percentage change from 2019 to 2021 on the model-implied nominal sectoral output changes. Column (4) relies on national accounts statistics from OECD-NAS, using sectoral nominal value added. We compute the annualized percentage change from 2019 to 2021 and regress it on the model-implied sectoral nominal output changes. Columns (1) and (2) are based on 16 sub-manufacturing industries from 21 European countries. Column (3) covers 35 sub-sectors across 27 countries. Column (4) uses data from 42 OECD countries. A complete list of countries is provided in Appendix Section B. The output growth values are aggregated from 2-digit OECD ISIC Rev. 4 codes to 1-digit NACE Rev. 2 sectors using value-added data from the OECD ICIO Tables. The 1-digit NACE sectors include A, B–E, F, G–I, J, K, L, and O–Q. Heteroskedasticity-robust standard errors are reported in parentheses. ***, **, and * indicate statistical significance at the 1% , 5%, and 10% levels, respectively.

In columns (1) and (2) of Table 8, the dependent variable is the actual sectoral output changes measured by the Eurostat-IP. In column (1) we test whether the actual shortages provided by EC-BCS is related to the observed output changes. In column (2), we use the model implied real output as the dependent variable. The statistically significant coefficient of interest, in both columns (1) and (2) as well as the reasonably high explanatory power of these regressions are both reassuring regarding the key mechanism in our model that

connects input shortages to output losses, at the same time confirming the close relation between actual sectoral output changes and the model-implied changes.

In columns (3) and (4) of Table 8, we evaluate our model's fit at the sectoral level using nominal output. For European countries, we utilize the Orbis firm-level database, released by Bureau van Dijk (BvD)—a Moody's Analytics company, where we aggregate firm-level gross output to sector level, in column (3). To check our aggregation and compare value added based output measure to gross output measure, we further use the "Value-added by Activity" data from OECD (2024) in column (4). Column (3) demonstrates a statistically significant positive correlation between our model-based sectoral output changes and nominal output changes based on firm-level data, with nearly 50% explanatory power. In column (4), we replicate the regression from column (3) across more countries but fewer sectors, resulting in reduced explanatory power but still a strong relationship. Note the similarity in the estimated coefficient across different columns, using different data.

Next, we focus on prices. Using input shortage data from EC-BCS, we examine whether sectors experiencing supply constraints and input shortages also exhibit higher prices. To investigate this relationship, we utilize national accounts statistics from Eurostat on the "Harmonized Index of Consumer Prices" (Eurostat-HICP). As documented by Eurostat (Eurostat-HCIP, 2024), this dataset covers 40 countries monthly, reporting at the Classification of Individual Consumption According to Purpose (COICOP) Group level (3-digits). However, data for the U.K. is unavailable post-Brexit, and the U.S. data lacks granularity at the 3-digit level. Additionally, some countries are absent in the ICIO data, leaving us with data from 30 countries for comparison purposes. To align COICOP groups with ICIO sectors, we manually match them and use item weights from 2019 provided by Eurostat-HCIP-2 (2024) in cases of many-to-one matching scenarios.

Figure E.5 illustrates the distribution of model-implied factor price changes across countries. Notably, sectors experiencing significant factor price increases (depicted in green) are predominantly those in tradable sectors, while services sectors show smaller changes (depicted in yellow and red). To relate the model-implied price changes to the actual input shortages observed, we utilize the data we have shown above in a regression framework. Table 9 presents the regression results. The dependent variable is the change in the severity of input shortages during the pandemic. Column (1) tests whether sectors with more pronounced input shortages tend to also experience higher wages. The positive and statistically significant coefficient that we estimate together with high R^2 supports this hypothesis. The findings in column (2) are similar and provide further supportive evidence: sectors experiencing significant input shortages, such as motor vehicles or electronics (as shown in

Figure C.3) tend to experience higher goods prices. The positive and significant coefficient confirms this relationship.

Table 9: EVALUATING MODEL FIT-II

Sample:	**EC-BCS**		**Eurostat-HICP**	
Dep Var (Data)	Input Shortage	Input Shortage	Price Change (%)	Price Change (%)
	(1)	(2)	(3)	(4)
%Δw (Model)	0.0406**		0.0711**	
	(0.020)		(0.026)	
%ΔP (Model)		0.1377***		0.1194**
		(0.039)		(0.042)
No. of Countries	21	21	30	30
No. of Sectors	16	16	12	12
Country FE	yes	yes	yes	yes
Obs.	282	282	359	359
R^2	0.34	0.35	0.30	0.30

NOTES: In columns (1) and (2), we measure the change in the severity of input shortages during the pandemic using the responses of business managers collected by the EC-BCS. These columns use data from 16 manufacturing industries across 21 European countries, focusing on changes observed during the pandemic period. In columns (3) and (4), we use price indices at the COICOP Group level (3-digit) for 30 European countries. The 3-digit COICOP Group categories are matched to 2-digit OECD ISIC Revision 4 codes using 3-digit item weights that we obtain from the Eurostat 2-digit OECD ISIC Revision 4 codes are 10to12, 13to15, 31to33, 35to39, 45to47, 49to53, 55to56, 64to66, 68, 85, 86to88. The list of countries are provided in Appendix Section B. Heteroskedastic-consistent standard errors are reported in parentheses. ***, **, and * indicate significance at the 1%, 5%, and 10% levels, respectively.

Columns (3) and (4) analyze the relationship between model-implied price changes and observed price changes from Eurostat-HICP data at the sector level. We find robust and significant correlations between actual price changes, represented by CPI data, and model-implied changes for both factor prices (column 3) and goods prices (column 4).

5 Conclusion

In the face of a global pandemic, the equitable distribution of vaccines transcends mere humanitarian duty; it is a strategic economic imperative. Our study underscores this by leveraging a structural model alongside economic and epidemiological data, demonstrating that scaling up vaccine production globally and ensuring universal access yields substantial eco-

nomic returns for advanced economies (AEs) that initially secured vaccines. This proactive investment offers AEs a remarkable 178 percent return on investment, mitigating not only their own economic downturns but also smoothing the broader global impact of the pandemic.

COVID-19 has delivered an unprecedented shock to the global economy, marked by a cascade of disparate demand and supply disruptions affecting nations at varying times. Unlike the synchronized impacts of previous crises such as the 2008-09 Global Financial Crisis, COVID-19's effects unfold asynchronously across borders due to recurring health shocks from evolving virus variants and disjointed international policy responses. Although the original shock was a common shock to health in all countries that initiated factory shutdowns and supply chain blockades, the disjointed international policies in health and other areas led to an even bigger fragmentation that has exacerbated the global supply chain bottlenecks and causing them to persist, driven by uneven vaccination rates and divergent economic stimuli among nations.

Our analysis employs a comprehensive global network model calibrated with sector-specific shocks across 65 countries and 35 sectors. These shocks, informed by epidemiological insights and national disease dynamics, illuminate how sectoral infections trigger localized lockdowns in the absence of widespread vaccination coverage. The resulting disruptions propagate through interconnected global trade and production networks, underscoring the criticality of vaccine equity in stabilizing international supply chains.

Early in the pandemic, global leaders such as WHO Director Dr. Tedros Ghebreyesus and European Commission President Dr. Ursula von der Leyen highlighted the imperative that "None of us will be safe until everyone is safe." Our findings extend this axiom into economic realms, illustrating that global recovery hinges on universal recovery. In essence, globalization acts both as an amplifier of shocks and a buffer against them, echoing John Donne's timeless observation that "No man is an island." Our study provides an economic corollary: "No economy is an island," emphasizing the interconnectedness of global economic stability and the imperative of equitable vaccine distribution in achieving it.

References

Allen, Linda JS, "A primer on stochastic epidemic models: Formulation, numerical simulation, and analysis," *Infectious Disease Modelling*, 2017, *2* (2), 128–142.

Atalay, Engin, "How important are sectoral shocks?," *American Economic Journal: Macroeconomics*, 2017, *9* (4), 254–80.

Atkeson, Andrew, "How Deadly is COVID-19? Understanding the Difficulties with Estimation of its Fatality Rate," Working Paper 26965, National Bureau of Economic Research 2020.

Baqaee, David and Emmanuel Farhi, "Supply and demand in disaggregated keynesian economies with an application to the COVID-19-19 crisis," *American Economic Review*, 2022, *112* (5), 1397–1436.

Baqaee, David Rezza and Emmanuel Farhi, "Networks, barriers, and trade," *Econometrica*, 2024, *92* (2), 505–541.

Boehm, Christoph E, Aaron Flaaen, and Nitya Pandalai-Nayar, "Input linkages and the transmission of shocks: Firm-level evidence from the 2011 Tōhoku earthquake," *Review of Economics and Statistics*, 2019, *101* (1), 60–75.

_ , Andrei A Levchenko, and Nitya Pandalai-Nayar, "The long and short (run) of trade elasticities," *American Economic Review*, 2023, *113* (4), 861–905.

BvD-Orbis, "Moody's Orbis Global Commercial Firm-level Database," 2023. https://www.moodys.com/web/en/us/datahub.html.

Çakmaklı, Cem and Yasin Şimşek, "Bridging the Covid-19 data and the epidemiological model using the time-varying parameter SIRD model," *Journal of Econometrics*, 2024, *242* (1), 105787.

Caliendo, Lorenzo and Fernando Parro, "Estimates of the Trade and Welfare Effects of NAFTA," *Review of Economic Studies*, 2015, *82* (1), 1–44.

Chetty, Raj, John N Friedman, Nathaniel Hendren, Michael Stepner, and The Opportunity Insights Team, "How Did COVID-19 and Stabilization Policies Affect Spending and Employment? A New Real-Time Economic Tracker Based on Private Sector Data," Working Paper 27431, National Bureau of Economic Research 2020.

Costinot, Arnaud and Andrés Rodríguez-Clare, "Trade theory with numbers: Quantifying the consequences of globalization," in "Handbook of International Economics," Vol. 4, Elsevier, 2014, pp. 197–261.

CPS, "U.S. Bureau of Labor Statistics: Current Population Survey," 2022. https://www.bls.gov/cps/home.htm.

Dekle, Robert, Jonathan Eaton, and Samuel Kortum, "Unbalanced Trade," *American Economic Review: Papers & Proceedings*, May 2007, *97* (2), 351–355.

di Giovanni, Julian, Şebnem Kalemli-Özcan, Alvaro Silva, and Muhammed Ali Yıldırım, "Global Supply Chain Pressures, International Trade, and Inflation," Working Paper 30240, National Bureau of Economic Research 2022.

Dingel, Jonathan I and Brent Neiman, "How many jobs can be done at home?," *Journal of Public Economics*, 2020, *189*, 104235.

EC-BCS, "European Commission: Business and Consumer Surveys," 2022. https://economy-finance.ec.europa.eu/economic-forecast-and-surveys/business-and-consumer-surveys/download-business-and-consumer-survey-data/time-series_en.

Eurostat-HCIP, "Eurostat: Harmonized Index of Consumer Prices, monthly data," 2024. https://ec.europa.eu/eurostat/databrowser/view/prc_hicp_manr/default/table?lang=en.

Eurostat-HCIP-2, "Eurostat: Harmonized Index of Consumer Prices, item weights," 2024. https://ec.europa.eu/eurostat/databrowser/view/PRC_HICP_INW/default/table?lang=en.

Eurostat-IP, "Eurostat: Industrial Production Index by Industry," 2022. https://ec.europa.eu/eurostat/databrowser/view/sts_inpr_m/default/table?lang=en&category=sts.sts_ind.sts_ind_prod.

Fauci, AS, HC Lane, and RR Redfield, "COVID-19-Navigating the Uncharted.," *The New England Journal of Medicine*, 2020, *382* (13), 1268–1269.

Fernald, John and Huiyu Li, "The Impact of COVID on Productivity and Potential Output," 2022. Jackson Hole Economic Symposium.

Fernández-Villaverde, Jesús and Charles I Jones, "Estimating and simulating a SIRD model of COVID-19 for many countries, states, and cities," *Journal of Economic Dynamics and Control*, 2022, p. 104318.

Goolsbee, Austan and Chad Syverson, "Fear, lockdown, and diversion: Comparing drivers of pandemic economic decline 2020," *Journal of Public Economics*, 2021, *193*, 104311.

Guerrieri, Veronica, Guido Lorenzoni, Ludwig Straub, and Iván Werning, "Macroeconomic Implications of COVID-19: Can Negative Supply Shocks Cause Demand Shortages?," *American Economic Review*, 2022, *112* (5), 1437–74.

Hortaçsu, Ali, Jiarui Liu, and Timothy Schwieg, "Estimating the fraction of unreported infections in epidemics with a known epicenter: An application to COVID-19," *Journal of Econometrics*, 2021, *220* (1), 106–129.

Horvàt, Peter, Colin Webb, and Norihiko Yamano, "Measuring employment in global value chains," 2020. https://www.oecd-ilibrary.org/content/paper/00f7d7db-en.

HPS, "U.S. Census Bureau: Household Pulse Survey," 2022. https://www.census.gov/programs-surveys/household-pulse-survey.html.

Kalemli-Özcan, Şebnem, Bent E Sørensen, Carolina Villegas-Sanchez, Vadym Volosovych, and Sevcan Yeşiltaş, "How to Construct Nationally Representative Firm-Level Data from the Orbis Global Database: New Facts on SMEs and Aggregate Implications for Industry Concentration," *American Economic Journal: Macroeconomics*, 2024, *16* (2), 353–374.

Krugman, Paul R, Maurice Obstfeld, and Marc Melitz, *International Economics: Theory and Policy*, Pearson, 2022.

Ledford, H, "COVID vaccine hoarding might have cost more than a million lives.," *Nature*, 2022.

Li, Ruiyun, Sen Pei, Bin Chen, Yimeng Song, Tao Zhang, Wan Yang, and Jeffrey Shaman, "Substantial undocumented infection facilitates the rapid dissemination of novel coronavirus (SARS-CoV2)," *Science*, 2020.

OECD, "OECD Inter-Country Input-Output (ICIO) Tables," 2020. https://www.oecd.org/sti/ind/inter-country-input-output-tables.htm.

_ , "OECD National Accounts Statistics," 2024. https://www.oecd-ilibrary.org/economics/data/oecd-national-accounts-statistics_na-data-en.

Vogel, Gretchen, "New blood tests for antibodies could show true scale of coronavirus pandemic," *Science*, March 19 2020.

APPENDIX

A The Epidemiological SIR Model

Let's take a population of size N. At any given time t, we can split the population into three classes of people: Susceptible (S_t), Infected (I_t), and Recovered (Rc_t). We provide the model for a single country, suppressing the country index for the ease of the demonstration.[20] The susceptible group does not yet have immunity to the disease, and the individuals in this group have the possibility of getting infected. The recovered group, on the other hand, consists of individuals who are immune to the disease. Immunity can be developed either because the individual goes through the infection or because they get vaccinated. The SIR model builds on the simple principle that a fraction of the infected individuals in the population, $\frac{I_{t-1}}{N}$, can transmit the disease to susceptible ones S_{t-1} with a (structural) infection rate of β. Therefore, the number of newly infected individuals in the current period is $\beta S_{t-1}\frac{I_{t-1}}{N}$. The newly infected individuals should be deducted from the pool of susceptible individuals in the current period. Meanwhile, in each period, a fraction γ of the infected people recover from the disease, which in turn reduces the number of actively infected individuals. To track any changes in the number of individuals in the above-mentioned three groups, the following set of difference equations are used:

$$\Delta S_t = -\beta S_{t-1}\frac{I_{t-1}}{N} \tag{A.1}$$

$$\Delta Rc_t = \gamma I_{t-1} \tag{A.2}$$

$$\Delta I_t = \beta S_{t-1}\frac{I_{t-1}}{N} - \gamma I_{t-1}. \tag{A.3}$$

The law of motion for the number of infected individuals shows the trajectory of the pandemic at the aggregate level. Note that, $\Delta S_t + \Delta Rc_t + \Delta I_t = 0$ holds at any given time, assuming that the size of the population remains constant.[21]

A central metric that characterizes the course of the pandemic is the basic reproduction number, denoted as R_0. The basic reproduction number refers to the speed of the diffusion, which can be computed by the ratio of newly infected individuals to the recovered cases. Therefore, it serves as a threshold parameter of many epidemiological models for

[20] We do not model cross-country infections due to travel as a source of prolonged pandemics.

[21] A small fraction of the resolved cases includes deaths due to disease, reducing the population size. In our setting, we suppress the fraction of death cases in the recovery rate parameter γ, assuming that the population remains fixed for the SIR model to remain tractable. Therefore, throughout the text, we use the terms "resolution rate" and "recovery rate" interchangeably for the parameter γ. See also Atkeson (2020), Fauci et al. (2020), Li et al. (2020), and Vogel (2020) on different estimates of recovery and death rates.

examining whether the disease will be extinct or spread further. Accordingly, using (A.1) and (A.2), R_0 is equal to β/γ assuming that $\frac{S(t)}{N} \approx 1$ at the onset of the pandemic. In this sense, a value of R_0 being less than unity indicates that the pandemic is contained, and if it exceeds unity, this implies that the spread of the pandemic continues.

We modify the canonical SIR model to allow for sectoral heterogeneity in terms of the size and working conditions that can lead to distinct infection trajectories in each sector. The transmission of the virus accelerates with close physical proximity. Hence, employees working in industries with higher physical proximity are infected with a higher probability. We assume that the economy is composed of K sectors. We denote the industries by subscript $i = 1, \ldots, K$. Each industry has L_i workers (since factors are industry-specific, we can index them with the industry index) and there is also the non-working population which we denote by N_{NW}. Each industry has two types of workers: (i) employees who can perform their jobs remotely (i.e., teleworkable) and (ii) employees who need to be on-site to fulfill their tasks. In each industry, we denote the number of employees in the first group with TW_i and the second group with N_i. Hence:

$$L_i = TW_i + N_i.$$

For the disease propagation, we lump the non-working population and the employees in the teleworkable jobs together and call them the "at-home" group. We denote the at-home group with index $i = 0$. The total number of individuals in this group is, therefore:

$$N_0 = N_{NW} + \sum_{i=1}^{K} TW_i.$$

Suppose that the infection rate in the at-home group is β_0. To account for heterogeneous physical proximities across industries, we compute the rate of infection for each industry i, denoted by β_i, as:

$$\beta_i = \beta_0 \text{Prox}_i \qquad \text{for} \quad i = 1, \ldots, K \tag{A.4}$$

where Prox_i is the proximity index for industry i that captures the contact intensive nature of the industry.

Here, $S_{i,t}$, $I_{i,t}$ and $Rc_{i,t}$ denote the number of susceptible, infected and recovered individuals, respectively, and $N_i = S_{i,t} + I_{i,t} + Rc_{i,t}$ denotes the total number of on-site individuals in industry i and the at-home group ($i = 0$). Susceptible individuals in the at-home group

can get infected from the infected individuals in the entire society:

$$\Delta S_{0,t} = -\beta_0 S_{0,t-1} \frac{I_{t-1}}{N},$$

where $I_t = \sum_{i=1}^{K} I_{i,t} + I_{0,t}$ captures the total number of infected individuals. An on-site worker in sector i, however, could be exposed to infection either at work, at the rate of $\beta_i S_{i,t-1} \frac{I_{i,t-1}}{N_i}$, or outside work, that involves all the remaining activities –including family life, shopping and commuting– at the rate $\beta_0 S_{i,t-1} \frac{I_{t-1}}{N}$. Hence, the number of susceptible individuals among the on-site workers in industry i changes as:

$$\Delta S_{i,t} = -\beta_i S_{i,t-1} \frac{I_{i,t-1}}{N_i} - \beta_0 S_{i,t-1} \frac{I_{t-1}}{N}.$$

The recovery rate is the same for all types of infected individuals:

$$\Delta Rc_{i,t} = \gamma I_{i,t-1}.$$

The number of infected individuals changes as the susceptible individuals get infected and some infected individuals recover from the disease:

$$\Delta I_{i,t} = -\left(\Delta Rc_{i,t} + \Delta S_{i,t}\right).$$

We can write the evolution of the infected individuals in terms of matrices as:

$$\boldsymbol{I}_t = \boldsymbol{I}_{t-1} + \text{diag}(\boldsymbol{S}_{t-1}/N)\, B\, \boldsymbol{I}_{t-1} - \gamma \boldsymbol{I}_{t-1} = \left[\text{diag}(\boldsymbol{S}_{t-1}/N)\, B - (1-\gamma)\mathcal{I}_{K+1}\right]\, \boldsymbol{I}_{t-1},$$

where $\boldsymbol{I}_t$ and $\boldsymbol{S}_t$ are $K+1$ dimensional vectors, diag creates a diagonal matrix, $\mathcal{I}_{K+1}$ is the identity matrix and B is a $(K+1) \times (K+1)$ dimensional matrix, whose elements are given by:

$$B = \begin{bmatrix} \beta_0 & \beta_0 & \dots & \dots & \beta_0 & \beta_0 \\ \beta_0 & \beta_0+\beta_1 & \beta_0 & \dots & \dots & \beta_0 \\ \beta_0 & \beta_0 & \beta_0+\beta_2 & \beta_0 & \dots & \beta_0 \\ \vdots & \vdots & & \ddots & & \vdots \\ \vdots & \vdots & & & \ddots & \vdots \\ \beta_0 & \beta_0 & \dots & \dots & & \beta_0+\beta_K \end{bmatrix}$$

In period t, the effective infection rate at time t (β^t) is given by:

$$\beta^t S_{t-1} \frac{I_{t-1}}{N} = \beta_0 S_{t-1} \frac{I_{t-1}}{N} + \sum_{i=1}^{K} \beta_i S_{i,t-1} \frac{I_{i,t-1}}{N_i}.$$

In our simulations, we match the employment size weighted average β_i's of the infected individuals to observed overall β in a country at the very beginning ($t = 1$) when $S_i \approx N_i$ and $I_i/N_i \approx I/N$ to initialize the system. Using Equation (A.4), we impose:

$$\beta = \beta_0 + \sum_{i=1}^{K} \beta_i \frac{N_i}{N} = \beta_0 + \beta_0 \sum_{i=1}^{K} \text{Prox}_i \frac{N_i}{N}$$

Hence, we solve for β_0 in terms of β, industry size, and the proximity levels as:

$$\beta_0 = \beta \left(1 + \sum_{i=1}^{K} \frac{\text{Prox}_i N_i}{N} \right)^{-1}. \tag{A.5}$$

B Data Details

B.1 Household Pulse Survey

The U.S. Census Bureau designed the Household Pulse Survey, henceforth HPS (see HPS, 2022), to understand the individuals' experiences of Covid-19 as well as to provide timely information essential in terms of employment status, food security, housing, physical and mental health, access to health care and educational disruption.[22]

For our analysis, we focus on the national-level information in terms of employment status that is available in the employment section.[23] This section asks the U.S. households the reasons for not working and counts the responses for each reason reported. Using the counts available, we first linearly interpolate the weekly/bi-weekly series into the daily series. We then group the reasons for not working into the following three categories, listed

[22] As of May 2022, the HPS had three phases: In Phase 1 U.S. households were surveyed on a *weekly basis* over the period from April 23, 2020 to July 21, 2020; In Phase 2 U.S. households were surveyed on a *bi-weekly basis* over the period from August 19, 2020 to October 26, 2020; In Phase 3, U.S. households were surveyed on a *bi-weekly basis* over the period from October 28, 2020 to May 9, 2022.

[23] The HPS uses a national representative sample to produce estimates at three geographic levels: (1) 15 largest Metropolitan Statistical Areas, (2) each of the 50 states plus the District of Columbia, and (3) the national level. Each round of HPS provides "Table 3. Educational Attainment for Adults Not Working at Time of Survey, by Main Reason for Not Working and Source Used to Meet Spending Needs."

below.

(i) **Individual pandemic related reasons (47.1%)**

- I was caring for someone or sick myself with coronavirus symptoms
- I did not work because I am/was caring for children not in school or daycare
- I was concerned about getting or spreading the coronavirus
- I did not work because I am/was caring for an elderly person
- I am/was sick (not coronavirus related) or disabled

(ii) **Business related reasons (15%)**

- I was laid off or furloughed due to coronavirus pandemic
- My employment went out of business due to the coronavirus pandemic

(iii) **Government mandated reasons (4.7%)**

- My employment closed temporarily due to the coronavirus pandemic

For reasons for not being employed, 47.1% of the U.S. population aged 18 years and older reported individual pandemic-related reasons, 15% reported business-related reasons and 4.7% reported government mandated reasons.[24]

B.2 Current Population Survey

The U.S. Bureau of Labor Statistics conducts the monthly household labor force survey, Current Population Survey, henceforth CPS (CPS, 2022), to track the number of employed people who missed work during the survey reference week. Specifically, this survey provides the following measures: i) people who did not work at all in the survey reference week, ii) people who usually work full time but were at work part-time (1 to 34 hours) during the reference week. Different from the HPS explained above, this survey provides time series data that goes until 2012. This feature enables us to compare post-Covid-19 employment figures with pre-Covid-19 ones. For our analysis, we utilize the time series data on

[24]From the total U.S. population, we excluded the households who stated the reason for not working as the retirement at the time of the survey. We calculate the shares by collapsing daily values into yearly values and taking the average of the resulting yearly responses over the period from 2020 to 2022. The numbers do not add up to 100 because the households stating the reason for not working as "Other" and "No response" are not considered in the computation.

Figure B.1: Reasons for Not Working, 2012m1–2022m7

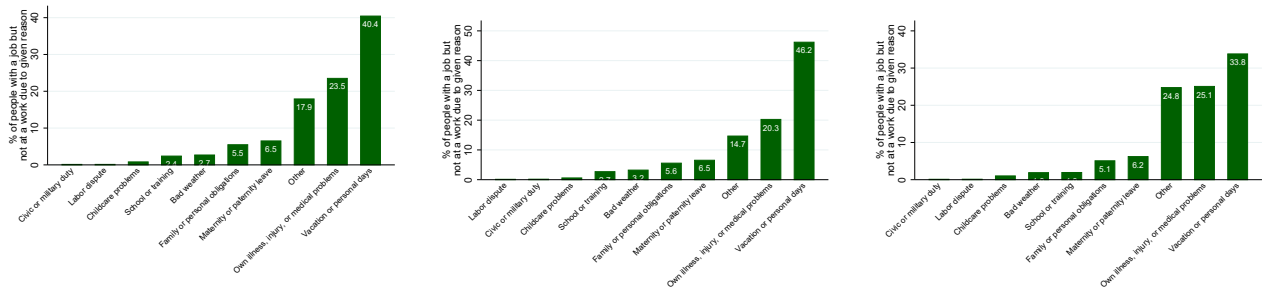

(a) averages over the sample period 2012m1-2022m7

(b) pre-Covid-19 averages

(c) post-Covid-19 averages

NOTES: Figure B.1 displays the fraction of "employed" households in each of the given categories, based on their expressed reasons for not being at work. The numbers may not be added up to 100 because of rounding in the computation of the corresponding averages.

employed people with a job not at work for selected reasons. Figure B.1 displays the fraction of "employed" households in each of the given categories, based on their expressed reasons for not being at work.

B.3 Data Sources for Empirical Validation

BvD-Orbis We utilize the Orbis database, a commercial product released by Bureau van Dijk (BvD)—a Moody's Analytics company. We download firm-level information from the Moody's DataHub, which is a cloud-based data delivery platform (BvD-Orbis, 2023). For our analysis, we adhere closely to the instructions and programs outlined in Online Appendix of Kalemli-Özcan et al. (2024). We follow their guidelines to construct and clean the firm-level samples of the selected 27 countries to ensure its quality and readiness for our empirical validation exercise. The included countries are: Austria (AT), Belgium (BE), Bulgaria (BG), Switzerland (CH), Czechia (CZ), Germany (DE), Denmark (DK), Estonia (EE), Spain (ES), Finland (FI), the United Kingdom (GB), Greece (GR), Croatia (HR), Hungary (HU), Ireland (IE), Iceland (IS), Italy (IT), Japan (JP), Kazakhstan (KZ), Lithuania (LT), Norway (NO), Portugal (PT), Romania (RO), Russian Federation (RU), Slovenia (SI), Slovakia (SK), and Turkey (TR).

OECD-NAS We use the "Value-added by Activity" data from OECD (2024). We aggregate our model output to match the level of sector aggregation present in this data set for 42 OECD countries. The included countries are: Australia (AU), Austria (AT), Belgium (BE),

Brazil (BR), Chile (CL), China (CN), Colombia (CO), Costa Rica (CR), Czechia (CZ), Germany (DE), Denmark (DK), Estonia (EE), Spain (ES), Finland (FI), France (FR), the United Kingdom (GB), Greece (GR), Hungary (HU), Ireland (IE), Iceland (IS), India (IN), Indonesia (ID), Israel (IS), Italy (IT), Japan (JP), South Korea (KR), Lithuania (LT), Luxembourg (LU), Latvia (LV), Mexico (MX), the Netherlands (NL), New Zealand (NZ), Norway (NO), Poland (PL), Portugal (PT), Slovenia (SI), Sweden (SE), Slovakia (SK), South Africa (ZA), Switzerland (CH), the United States (US), and Turkey (TR).

Eurostat IP We use the "Industrial Production Index by Industry" data that is provided by Eurostat-IP (2022) for 21 EU member countries on a monthly basis. We aggregate 24 manufacturing sub-industries (classified based on NACE Revision 2 Industry Codes) to corresponding 16 sub-manufacturing sectors (classified according to ISIC Revision 4 in the OECD-ICIO data) using sectoral production values as weights. The included countries are: Austria (AT), Belgium (BE), Bulgaria (BG), Czechia (CZ), Germany (DE), Denmark (DK), Estonia (EE), Spain (ES), Finland (FI), France (FR), Hungary (HU), Ireland (IE), Italy (IT), Lithuania (LT), Latvia (LV), the Netherlands (NL), Poland (PL), Portugal (PT), Romania (RO), Sweden (SE), and Turkey (TR).

Eurostat HICP We use the "Harmonised Index of Consumer Prices (HICP)" data that is provided by Eurostat-HCIP (2024) for 40 countries on a monthly basis reported at Classification of Individual Consumption According to Purpose (COICOP) Group level (3-digits). However, the data for U.K. is not available after Brexit and the data for U.S. is not available at 3-digit level. And some countries are absent in ICIO data, which gives us 30 countries to do the comparison. We matched COICOP groups to ICIO sectors manually and used item weights from 2019 provided by Eurostat-HCIP-2 (2024) when there is a many to one matching. The included countries are: Austria (AT), Belgium (BE), Bulgaria (BG), Croatia (HR), Cyprus (CY), Czechia (CZ), Germany (DE), Denmark (DK), Estonia (EE), Spain (ES), Finland (FI), France (FR), Hungary (HU), Ireland (IE), Iceland (IS), Italy (IT), Lithuania (LT), Latvia (LV), Luxembourg (LU), Malta (MT), the Netherlands (NL), Norway (NO), Poland (PL), Portugal (PT), Romania (RO), Slovenia (SI), Sweden (SE), Slovakia (SK), Switzerland (CH) and Turkey (TR).

EC-BCS We use the survey-based time series data provided by EC-BCS (2022). The survey currently covers all 27 EU Member States and all five EU candidate countries (i.e. Montenegro, North Macedonia, Albania, Serbia and Turkey). The respective survey conducted by

European Commission on a quarterly basis to ask business managers of those countries on the factors limiting production. For our purpose, we utilize the responses of managers from 24 manufacturing sub-industries (classified based on NACE Revision 2 Industry Codes).

C Empirical Evidence

In this section, we provide additional empirical evidence using the time series data provided by EC-BCS. Panel A of Figure C.2 plots these factors as a weighted average of all EU countries for manufacturing, construction, and services sectors. Historically, especially during the 2008–2009 crisis, we observe that insufficient demand (blue line) is the most important factor limiting production. During times of low demand, labor and/or material shortages turn out to be nonbinding constraints. This is consistent with the intuition that when the economy is demand-constrained, there is a limited role for supply chain bottlenecks. What is unique about the Covid-19 shock is the shortage of material and equipment (the green line), and labor (red line) which both became the key reasons for limiting production in all sectors, including services.

Figure C.2: Factors Limiting Production in Europe

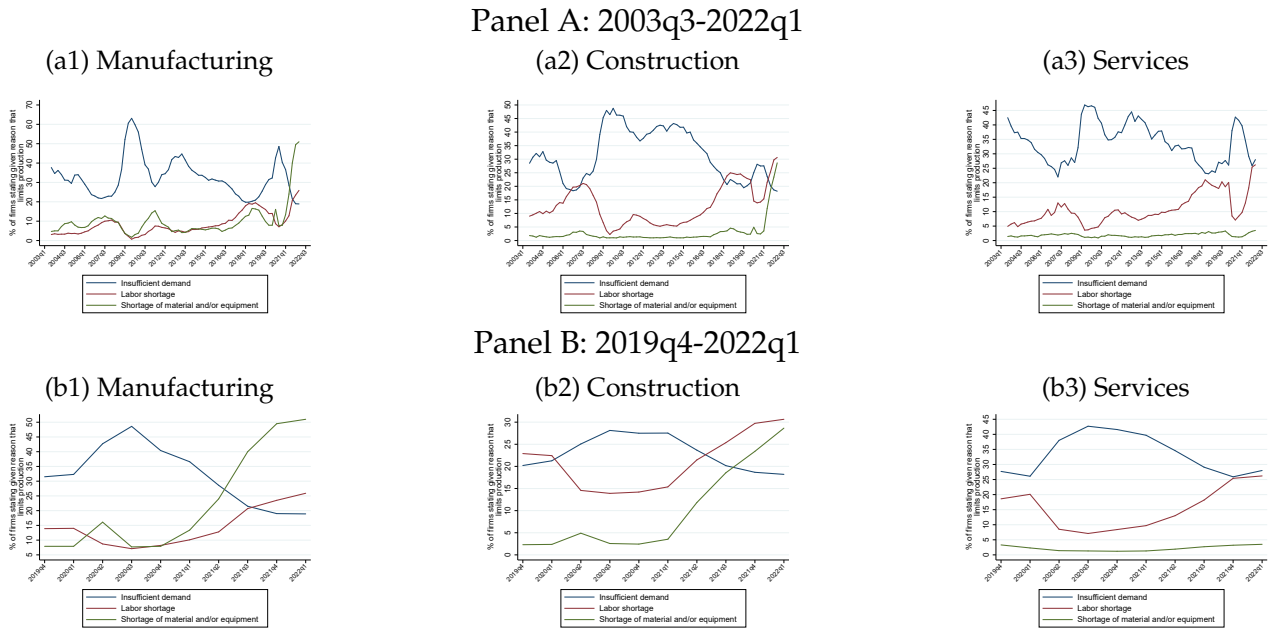

NOTES: Figure C.2 plots the replies of business managers to the question "What main factors are currently limiting your production?" as a weighted average using country shares in EU's total gross value added. These series are smoothed by calculating a two-year moving average and they are seasonally adjusted.

Figure C.2 also plots the period after 2019.Q4 to zoom in on the asymmetric dynamics

across sectors. As can be seen from Panel B of this figure, the recovery of demand, thanks to vaccinations and economic stimulus packages, worsened the labor and material shortages throughout 2021. This is consistent with the framework depicted in Guerrieri et al. (2022), which notes the asymmetric nature of the pandemic and the associated spillovers among sectors. Manufacturing, a tradeable sector, registered higher shortages of inputs due to the overlap of supply chain bottlenecks and recovery in demand. The adverse effects of the pandemic were rather noticeable in this sector because most of its inputs are imported. In comparison, non-tradeable sectors such as construction and services suffer relatively more from labor shortages. Given the complementarity of intermediate inputs and labor in our framework, our estimates can capture this notion of switching from a primarily demand-constrained world to a mostly supply-constrained world during the pandemic's course.

An analogous survey for the U.S. illustrates the factors limiting production as shown in Figure C.4. This figure highlights the importance of global supply chain bottlenecks even in the non-tradeable sectors of construction and services in panels (a2) & (b2) and (a3) & (b3), with the most important delays coming from foreign suppliers.

Figure C.3 digs deeper and provides a disaggregated picture of 2021.Q4 when material and/or equipment shortages stood out among the reported factors limiting the production in the EU manufacturing industry. In the heat map, the shades of red correspond to the extent of severity of material and/or equipment shortages in 2021.Q4 across different country-sector pairs. Darker shades of red correspond to more severity in shortages.

A comparison across the sectors shown in the rows reveals that those sectors that are more exposed to the "chip crisis", such as motor vehicles, computers, electrical equipment, machinery, and equipment, are generally more severely hit by supply chain disruptions, while clothing or petroleum products are less affected. A comparison across countries shown in the columns reveals that countries such as Germany, Italy, Denmark, and the Netherlands are hardest hit by these manufacturing bottlenecks.

The evidence presented here highlights the adverse effects of the pandemic on different sectors of the economy and various countries in a heterogeneous manner. This heterogeneity stems from the varying levels of exposure to the pandemic's impacts, including weak demand and supply chain disruptions. Different countries and sectors have experienced these challenges to differing degrees, reflecting their specific vulnerabilities and resilience.

Figure C.3: Cross-sector Heterogeneity in Shortage of Material and/or Equipment in in 2021Q4

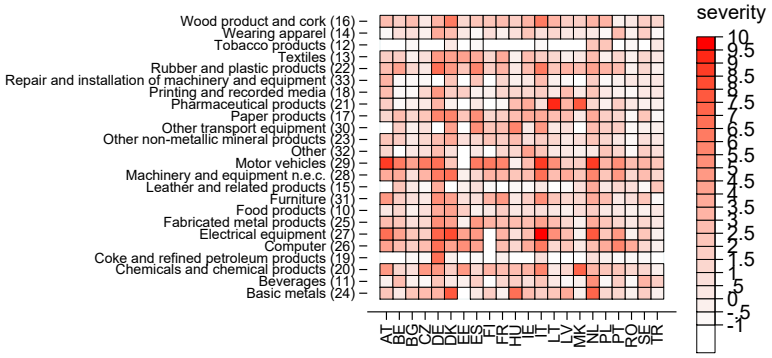

NOTES: Figure C.3 presents a heat map of shortages in the manufacturing industry in 2021Q4. The shades of red correspond to the varying extent of severity. The extent of severity for a given country-sector pair is measured by the standard deviation of the positive responses to the EC-BCS's question "*the shortage of material and/or equipment is a key limiting factor for their production*" exceeding the historical average. Empty boxes correspond to missing values. y-axis lists sub-sectors in the manufacturing industry with 2-digit Eurostat NACE Revision 2 industry codes in parentheses. x-axis lists the following countries: Austria (AT), Belgium (BE), Bulgaria (BG), Denmark (DE), Estonia (EE), Spain (ES), Finland (FI), France (FR), Hungary (HU), Ireland (IE), Italy (IT), Lithuania (LT), Latvia (LV), Macedonia (MK), the Netherlands (NL), Poland (PL), Portugal (PT), Romania (RO), Sweden (SE), and Turkey (TR).

D Sectoral Shocks with Sector Specific Labors

In this section, we provide an intuitive perspective to illustrate our results using a stylized two-sector economy. Figure D.5 shows the Production Possibility Frontiers (PPF) and the indifference curves of the economy under different scenarios. Before Covid-19, PPF was denoted by the blue line, and the utility maximization by the indifference curve was denoted by the black curve, yielding an equilibrium at point A. For this PPF, we assume that the labor is mobile between the sectors. Once we make the labor supply sector specific, we arrive at the PPF represented by the dashed blue line. The dashed blue PPF lies below the pre-Covid (solid blue) PPF. This is because the dashed line corresponds to the case with an additional constraint of immobile factor (see, e.g., the specific factors model in Chapter 4 of Krugman et al., 2022). Up to this stage, the equilibrium remains intact at pre-Covid equilibrium, point A. After we introduce a sectoral demand shock, however, the utility function changes such that we would be optimizing along the red indifference curves. If the labor was not sector-specific, the equilibrium would have moved to point B following the demand shock. Instead, the new equilibrium moves to point C. Furthermore, since there is also a labor supply shock in both sectors, the new PPF shifts inwards to the one represented

Figure C.4: Factors Limiting Production during the Pandemic in the U.S. (August 2020-May 2022)

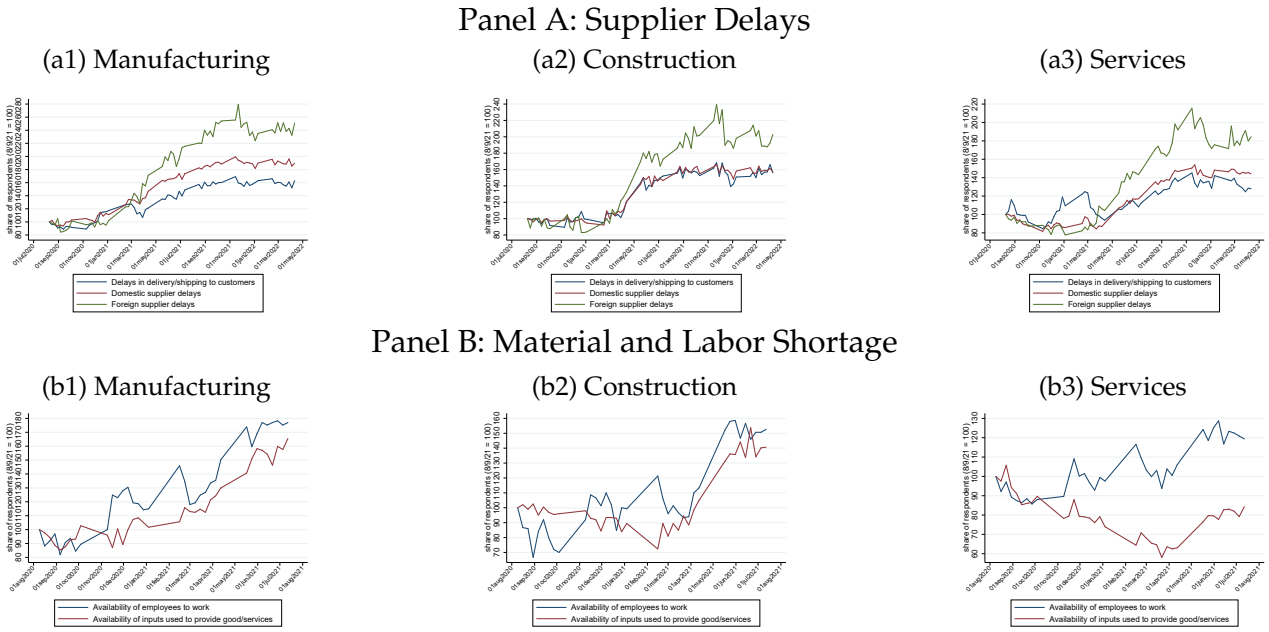

NOTES: Figure C.4 plots the replies of small business managers in the U.S. Pulse Survey to the question "In the last week, was this business affected by any of the following?" This figure provides a cross-sectoral comparison of the factors that limit U.S. production during the Covid-19 era.

Figure D.5: Sectoral Shocks and Production Possibility Frontier

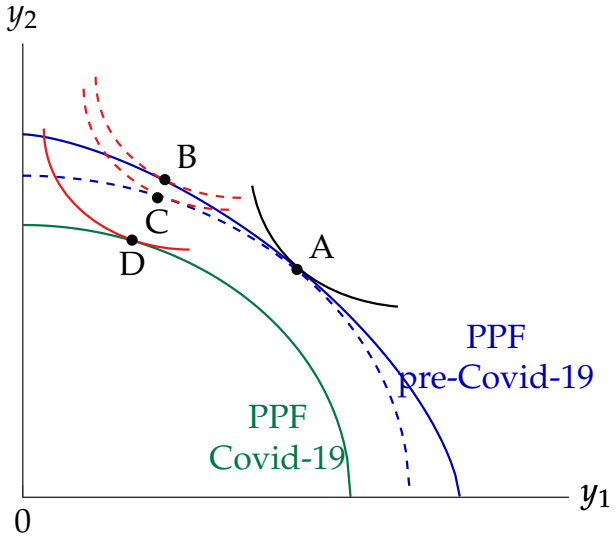

by the green line and the equilibrium moves to point D. With standard assumptions on indifference curves, one can deduce that the output in point D is lower than point C, which is lower than point B. In standard models, pure demand shocks as moving from point A to point B will not deliver real output effects. But since point C and point D are worse off compared to point B, point C is worse off than point B. To quantitatively compare the real output levels between points A and C, we use the Törnqvist index.

E Additional Figures and Tables

List of Figures and Tables:

- **Figure E.1:** The Structure of OECD Inter-Country Input-Output (ICIO) Table
- **Figure E.2:** Model Schematic with Nested Constant Elasticity of Substitution (CES)
- **Figure E.3:** Proximity Index and Teleworkable Share by Industry
- **Figure 6:** Labor Supply Shocks
- **Figure 7:** Demand Shocks
- **Figure E.4:** Real GDP Growth Comparison
- **Figure E.5:** Distribution of Factor Price Changes

- **Table E.1:** Country Settings for Various Scenarios
- **Table E.2:** ICU Bed Capacities
- **Table E.3:** List of Essential Sectors during Lockdowns
- **Table E.4:** Model-Implied Real Expenditure Losses Relative to the Pre-Pandemic World (percent): No Endogenous Lockdowns
- **Table 3:** Model-Implied Real Expenditure Losses Relative to the Pre-Pandemic World (percent): The Role of Vaccine Transfers

Figure E.1: THE STRUCTURE OF OECD INTER-COUNTRY INPUT-OUTPUT TABLE

	Intermediate use country 1 x industry 1 [...] country 65 x industry 36	**Final Demand** country 1 x fd 1 [...] country 65 x fd 7	**Output**
country 1 x industry 1 country 1 x industry 2 ... ... country 65 x industry 1 ... country 65 x industry 36	**(Z)**	**(F)**	**(Y)**
Value added + taxes - subsidies on intermediate products	**(VA)**		
Output	**(Y)**		

NOTES: This figure illustrates the structure of OECD Inter-Country Input-Output Table (ICIO), which represents the breakdown of output corresponding to 36 industries and 65 countries, giving us a matrix of 2340×2340 entries. In any industry-country combination, the output (Y) equals intermediate use (Z) plus final demand (F) of 36 industries in 65 countries. The industry list can be found in Figure E.3. Further, in any industry-country combination, final demand sums the following components of expenditures over 65 countries. fd1: Households Final Consumption Expenditure (HFCE); fd2: Non-Profit Institutions Serving Households (NPISH); fd3: General Government Final Consumption (GGFC); fd4: Gross Fixed Capital Formation (GFCF); fd5: Change in Inventories and Valuables (INVNT); fd6: Direct purchases by non-residents (NONRES); fd7: Statistical Discrepancy (DISC).

Figure E.2: Model Schematic with Nested Constant Elasticity of Substitution (CES)

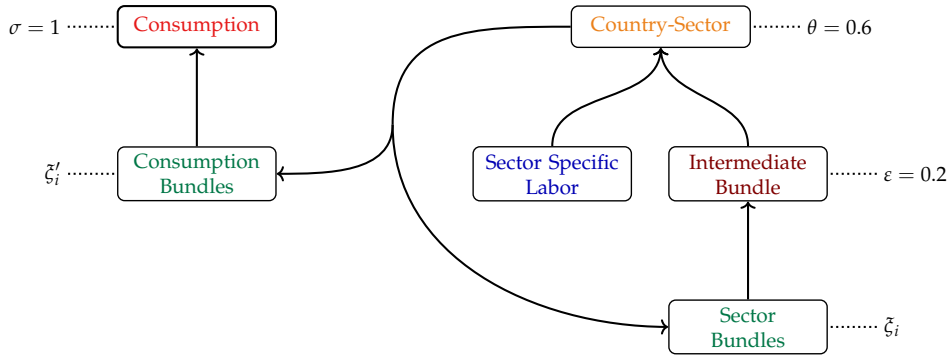

Figure E.3: Proximity Index and Teleworkable Share by Industry

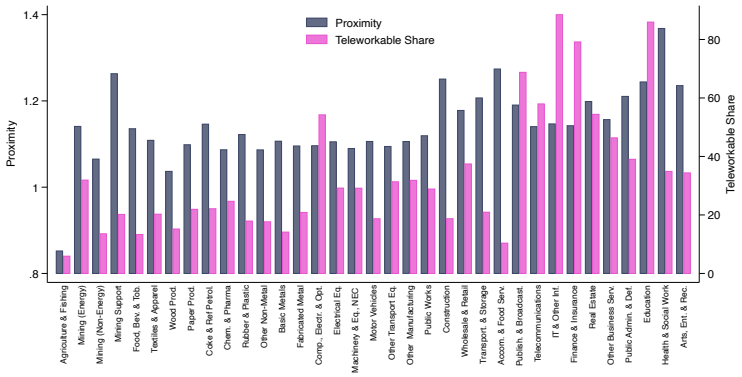

NOTES: In this figure, we present the physical proximity index, the share of teleworkable employees as well as demand changes in a given industry, which is categorized based on OECD ISIC Codes. In comparing proximity values across differential sectors listed in the first column, we use the weighted average of occupation-specific proximity values in those sectors. Specifically, an occupation of a given industry is assigned a proximity value that is smaller than 1 if it has sparse working conditions. An occupation of a given industry is assigned a proximity value that is larger than 1 if it requires closer proximity than the "shared office" level. We calculate the proximity values for a given industry after removing the teleworkable share of the employees of that industry. Doing so, we follow Dingel and Neiman (2020)'s list of teleworkable occupations to determine the share of employees that can work remotely in each industry.

Figure E.4: Model vs Data

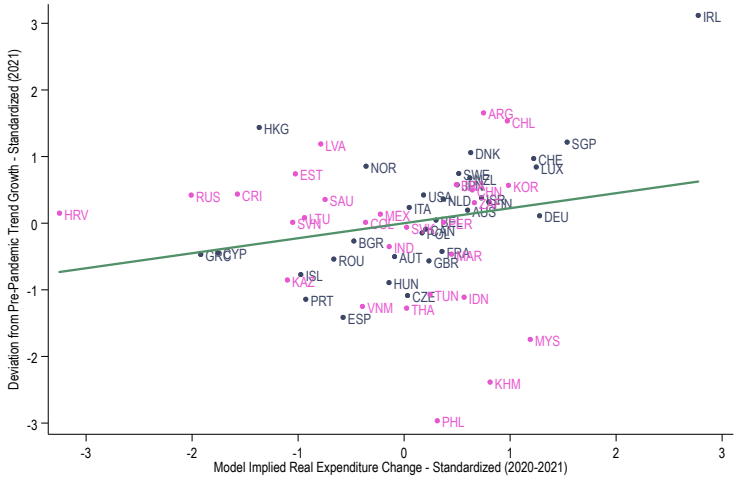

NOTES: This figure compares standardized changes in real GDP from 2020–2021: observed outcomes versus model-implied outcomes under the baseline scenario. Values are z-scores (each series is demeaned and divided by its standard deviation). The sample excludes Malta and Brunei (small economies) and Turkey (unconventional macroeconomic policies). Advanced economies (AEs) are shown in dark blue; emerging market and developing economies (EMDEs) in purple. The correlation between observed and model-implied growth is 23% for the full sample, 39% when the Philippines, Malaysia, and Cambodia are excluded, and 63% for AEs only. Source: World Development Indicators (World Bank) and authors' calculations.

Figure E.5: Factor Price Changes

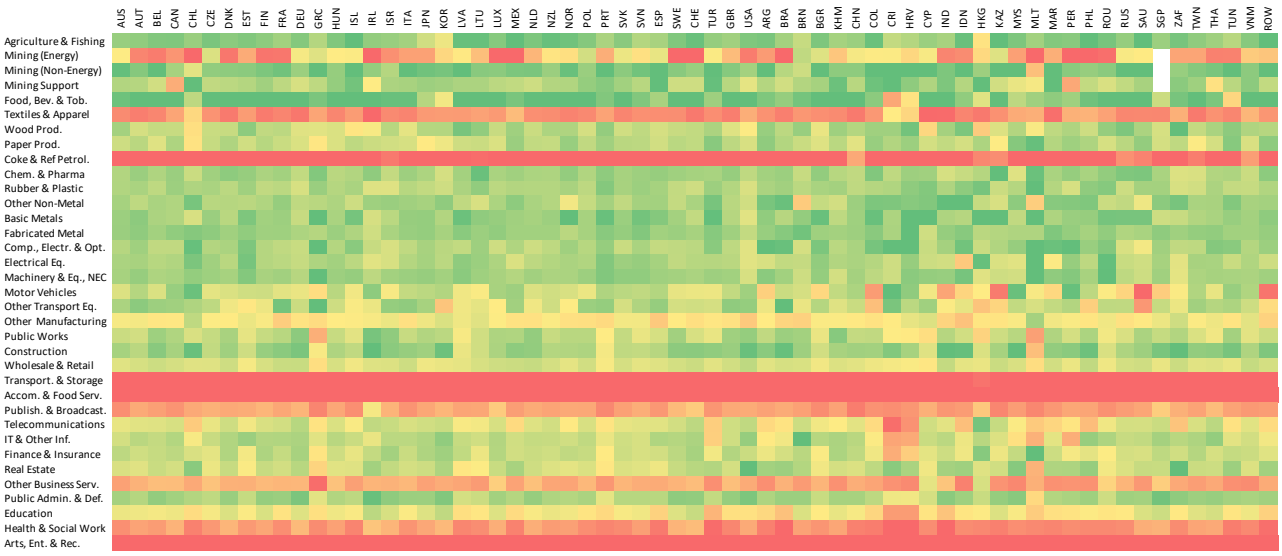

NOTES: Factor price changes from the Model. We calculate the z-scores for prices by subtracting the mean changes and dividing by the standard deviation of the changes within a country. Changes in prices are shown in the figure, ranging from a price decline relative to the mean, represented by red (starting from one standard deviation below) to prices aligned with the mean, represented by yellow (0), to price increases relative to the mean, represented by green (corresponding to one standard deviation above). Note that the order of countries is same as Table E.1.

Table E.1: Country Settings for Various Scenarios

Country	ICU capacity for Covid-19 patients	Reproduction rate R_0	GDP 2019 (Billion USD)	Share of vaccinated population	Duration of vaccination (days)	Openness Index
Australia	1665	0.7	1,393	100%	120 (30-90)	35
Austria	1000	1.1	446	100%	120 (30-90)	81
Belgium	2756	1.1	530	100%	120 (30-90)	164
Canada	2713	1.3	1,736	100%	120 (30-90)	52
Chile	1383	1.3	282	50%	330	49
Czechia	4151	1.1	247	100%	120 (30-90)	153
Denmark	925	1.2	348	100%	120 (30-90)	60
Estonia	338	1.2	31	100%	120 (30-90)	109
Finland	220	1.1	269	100%	120 (30-90)	55
France	8000	1.1	2,716	100%	120 (30-90)	45
Germany	28000	1.1	3,846	100%	120 (30-90)	71
Greece	704	1.1	210	100%	120 (30-90)	48
Hungary	1094	1.1	161	100%	120 (30-90)	151
Iceland	163	1.1	24	100%	120 (30-90)	49
Ireland	248	1.1	389	100%	120 (30-90)	69
Israel	4900	1.3	395	100%	120 (30-90)	34
Italy	7700	1.1	2,001	100%	120 (30-90)	50
Japan	3996	1.3	5,082	100%	120 (30-90)	28
Korea	5481	1.3	1,642	100%	120 (30-90)	64
Latvia	186	1.1	34	100%	120 (30-90)	102
Lithuania	451	1.1	54	100%	120 (30-90)	127
Luxembourg	91	1.1	71	100%	120 (30-90)	57
Mexico	4211	1.1	1,258	50%	330	74
Netherlands	1161	1.1	909	100%	120 (30-90)	148
New Zealand	585	0.7	207	100%	120 (30-90)	40
Norway	455	1.1	403	100%	120 (30-90)	47
Poland	3074	1.1	592	100%	120 (30-90)	89
Portugal	455	1.1	238	100%	120 (30-90)	66
Slovakia	570	1.1	105	100%	120 (30-90)	170
Slovenia	377	1.1	54	100%	120 (30-90)	166
Spain	4566	1.1	1,394	100%	120 (30-90)	51
Sweden	365	1.1	531	100%	120 (30-90)	60
Switzerland	1012	1.1	703	100%	120 (30-90)	84
Turkey	16850	1.3	754	50%	330	52
United Kingdom	7018	1.1	2,827	100%	120 (30-90)	41
US	84676	1.1	21,370	100%	120 (30-90)	20
Argentina	8404	1.1	450	50%	330	25
Brazil	43466	1.1	1,840	50%	330	22
Brunei	57	1.1	13	50%	330	90
Bulgaria	1347	1.1	68	100%	120 (30-90)	104
Cambodia	495	1.1	27	50%	330	131
China	50328	0.6	14,340	100%	120 (30-90)	32
Colombia	5286	1.3	324	50%	330	28
Costa Rica	136	1.1	62	50%	330	45
Croatia	277	1.3	60	50%	330	75
Cyprus	126	1.1	25	100%	120 (30-90)	51
India	32784	1.3	2,875	50%	330	28
Indonesia	7306	1.1	1,119	50%	330	30
Hong Kong	533	1.3	366	100%	120 (30-90)	304
Kazakhstan	3943	1.1	180	50%	330	53
Malaysia	1086	1.3	365	50%	330	122
Malta	70	1.1	15	100%	120 (30-90)	68
Morocco	2100	1.3	119	50%	330	67
Peru	943	1.1	227	50%	330	40
Philippines	2378	1.1	377	50%	330	49
Romania	1500	1.1	250	100%	120 (30-90)	69
Russia	17500	1.1	1,700	100%	120 (30-90)	40
Saudi Arabia	7813	1.1	793	50%	330	52
Singapore	650	1.2	372	100%	120 (30-90)	202
South Africa	2323	1.1	351	50%	330	56
Taiwan	6725	1.1	611	50%	330	101
Thailand	7241	1.1	544	50%	330	89
Tunisia	479	1.1	39	50%	330	94
Vietnam	251	1.1	262	50%	330	198
ROW	57225	1.1	7,276	50%	330	48

Notes: This table reports the ICU capacities (see Table E.2 for details), estimated reproduction rates, GDP figures (obtained from World Development Indicators, 2019 current dollars), shared of the population getting the vaccine (for scenario 3), duration of vaccination days (for scenario 3) and openness index, which is defined as the ratio of imports and exports to GDP.

Table E.2: ICU BED CAPACITIES

ISO-3	Country	ICU Covid-19	Reference
AUS	Australia	1665	https://www.mja.com.au/journal/2020/surge-capacity-australian-intensive-care-units-associated-covid-19-admissions
AUT	Austria	1000	https://www.covid19healthsystem.org/countries/austria/livinghit.aspx?Section=2.1%20Physical%20infrastructure&Type=Section
BEL	Belgium	2756	https://www.covid19healthsystem.org/countries/belgium/livinghit.aspx?Section=2.1%20Physical%20infrastructure&Type=Section
CAN	Canada	2713	https://www.covid19healthsystem.org/countries/canada/livinghit.aspx?Section=2.1%20Physical%20infrastructure&Type=Section
CHL	Chile	1383	https://www.oecd.org/coronavirus/en/data-insights/intensive-care-beds-capacity
CZE	Czech Republic	4151	https://www.covid19healthsystem.org/countries/czechrepublic/livinghit.aspx?Section=2.1%20Physical%20infrastructure&Type=Section
DNK	Denmark	925	https://www.sst.dk/-/media/Nyheder/2020/ITA_COVID_19_220320.ashx?la=da&hash=633349284353F4D8559B231CDA64169D327F1227
EST	Estonia	338	https://www.ncbi.nlm.nih.gov/pmc/articles/PMC7472675/
FIN	Finland	220	https://www.covid19healthsystem.org/countries/finland/livinghit.aspx?Section=2.1%20Physical%20infrastructure&Type=Section
FRA	France	8000	https://www.covid19healthsystem.org/countries/france/livinghit.aspx?Section=2.1%20Physical%20infrastructure&Type=Section
DEU	Germany	28000	https://www.covid19healthsystem.org/countries/germany/livinghit.aspx?Section=2.1%20Physical%20infrastructure&Type=Section
GRC	Greece	704	https://www.covid19healthsystem.org/countries/greece/livinghit.aspx?Section=2.1%20Physical%20infrastructure&Type=Section
HUN	Hungary	1094	https://www.oecd.org/coronavirus/en/data-insights/intensive-care-beds-capacity
ISL	Iceland	163	https://europepmc.org/article/med/32796182
IRL	Ireland	248	https://www.thejournal.ie/icu-bed-numbers-5217685-Sep2020/
ISR	Israel	4900	https://www.covid19healthsystem.org/countries/israel/livinghit.aspx?Section=2.1%20Physical%20infrastructure&Type=Section
ITA	Italy	7700	https://apnews.com/article/international-news-virus-outbreak-italy-barcelona-france-d7a43368a17f0abaff4d563151b84127
JPN	Japan	3996	https://journals.lww.com/ccmjournal/Fulltext/2020/05000/Critical_Care_Bed_Capacity_in_Asian_Countries_and.6.aspx
KOR	Korea, Rep.	5481	https://journals.lww.com/ccmjournal/Fulltext/2020/05000/Critical_Care_Bed_Capacity_in_Asian_Countries_and.6.aspx
LVA	Latvia	186	https://www.covid-19.no/critical-care-bed-numbers-in-europe
LTU	Lithuania	451	https://www.ncbi.nlm.nih.gov/pmc/articles/PMC7472675/
LUX	Luxembourg	91	https://www.ncbi.nlm.nih.gov/pmc/articles/PMC7472675/
MEX	Mexico	4211	https://www.oecd.org/coronavirus/en/data-insights/intensive-care-beds-capacity
NLD	Netherlands	1161	https://www.oecd.org/coronavirus/en/data-insights/intensive-care-beds-capacity
NZL	New Zealand	585	https://www.nzherald.co.nz/nz/covid-19-coronavirus-new-zealands-intensive-care-unit-capacity-revealed/GYQ2FXOYHJECZAHU2YKHXYFWXI/
NOR	Norway	455	https://www.oecd.org/coronavirus/en/data-insights/intensive-care-beds-capacity
POL	Poland	3074	https://www.ncbi.nlm.nih.gov/pmc/articles/PMC7472675/
PRT	Portugal	455	https://www.covid-19.no/critical-care-bed-numbers-in-europe
SVK	Slovak Republic	570	https://www.ncbi.nlm.nih.gov/pmc/articles/PMC7472675/
SVN	Slovenia	377	https://www.ncbi.nlm.nih.gov/pmc/articles/PMC7472675/
ESP	Spain	4566	https://www.covid-19.no/critical-care-bed-numbers-in-europe
SWE	Sweden	365	https://www.ncbi.nlm.nih.gov/pmc/articles/PMC7472675/
CHE	Switzerland	1012	https://www.oecd.org/coronavirus/en/data-insights/intensive-care-beds-capacity
TUR	Turkey	16850	https://dosyasb.saglik.gov.tr/Eklenti/36164,siy2018en2pdf.pdf?0
GBR	United Kingdom	7018	https://www.oecd.org/coronavirus/en/data-insights/intensive-care-beds-capacity
USA	United States	84676	https://www.oecd.org/coronavirus/en/data-insights/intensive-care-beds-capacity
ARG	Argentina	8404	https://www.oecd-ilibrary.org/sites/63d94877-en/index.html?itemId=/content/component/63d94877-en
BRA	Brazil	43466	https://www.oecd-ilibrary.org/sites/63d94877-en/index.html?itemId=/content/component/63d94877-en
BRN	Brunei Darussalam	57	https://journals.lww.com/ccmjournal/Fulltext/2020/05000/Critical_Care_Bed_Capacity_in_Asian_Countries_and.6.aspx
BGR	Bulgaria	1347	https://www.covid19healthsystem.org/countries/bulgaria/livinghit.aspx?Section=2.1%20Physical%20infrastructure&Type=Section
KHM	Cambodia	495	Selected to be close to the minimum observed levels.
CHN	China	50328	https://journals.lww.com/ccmjournal/Fulltext/2020/05000/Critical_Care_Bed_Capacity_in_Asian_Countries_and.6.aspx
COL	Colombia	5286	https://www.oecd-ilibrary.org/sites/63d94877-en/index.html?itemId=/content/component/63d94877-en
CRI	Costa Rica	136	https://www.oecd-ilibrary.org/sites/63d94877-en/index.html?itemId=/content/component/63d94877-en
HRV	Croatia	277	https://www.ncbi.nlm.nih.gov/pmc/articles/PMC7472675/
CYP	Cyprus	126	https://in-cyprus.philenews.com/coronavirus-seven-patients-in-intensive-care/
IND	India	32784	https://journals.lww.com/ccmjournal/Fulltext/2020/05000/Critical_Care_Bed_Capacity_in_Asian_Countries_and.6.aspx
IDN	Indonesia	7306	https://journals.lww.com/ccmjournal/Fulltext/2020/05000/Critical_Care_Bed_Capacity_in_Asian_Countries_and.6.aspx
HKG	Hong Kong SAR, China	533	https://journals.lww.com/ccmjournal/Fulltext/2020/05000/Critical_Care_Bed_Capacity_in_Asian_Countries_and.6.aspx
KAZ	Kazakhstan	3943	https://journals.lww.com/ccmjournal/Fulltext/2020/05000/Critical_Care_Bed_Capacity_in_Asian_Countries_and.6.aspx
MYS	Malaysia	1086	https://journals.lww.com/ccmjournal/Fulltext/2020/05000/Critical_Care_Bed_Capacity_in_Asian_Countries_and.6.aspx
MLT	Malta	70	https://www.covid19healthsystem.org/countries/malta/livinghit.aspx?Section=2.1%20Physical%20infrastructure&Type=Section
MAR	Morocco	2100	https://northafricapost.com/39786-covid-19-morocco-expands-hospital-capacity.html
PER	Peru	943	https://www.oecd-ilibrary.org/sites/63d94877-en/index.html?itemId=/content/component/63d94877-en
PHL	Philippines	2378	https://journals.lww.com/ccmjournal/Fulltext/2020/05000/Critical_Care_Bed_Capacity_in_Asian_Countries_and.6.aspx
ROU	Romania	1500	https://www.covid19healthsystem.org/countries/romania/livinghit.aspx?Section=2.1%20Physical%20infrastructure&Type=Section
RUS	Russian Federation	17500	https://tass.com/world/1162077
SAU	Saudi Arabia	7813	https://journals.lww.com/ccmjournal/Fulltext/2020/05000/Critical_Care_Bed_Capacity_in_Asian_Countries_and.6.aspx
SGP	Singapore	650	https://journals.lww.com/ccmjournal/Fulltext/2020/05000/Critical_Care_Bed_Capacity_in_Asian_Countries_and.6.aspx
ZAF	South Africa	2323	https://www.samrc.ac.za/news/covid-19-surge-investing-heavily-icu-capacity-not-only-option
TWN	Taiwan	6725	https://journals.lww.com/ccmjournal/Fulltext/2020/05000/Critical_Care_Bed_Capacity_in_Asian_Countries_and.6.aspx
THA	Thailand	7241	https://journals.lww.com/ccmjournal/Fulltext/2020/05000/Critical_Care_Bed_Capacity_in_Asian_Countries_and.6.aspx
TUN	Tunisia	479	https://www.medrxiv.org/content/10.1101/2020.06.02.20120147v1.full.pdf
VNM	Vietnam	251	https://www.who.int/docs/default-source/wpro---documents/countries/viet-nam/covid-19/vnm-moh-who-covid-19-sitrep4.pdf
ROW	Rest of the World	57225	Selected to be close to the minimum observed levels.

NOTES: This table provides the resources from which we built the ICU capacities dedicated to Covid-19 patients in each country. If there is a direct number for the ICU beds for Covid-19 in a resource, we used that number. Otherwise, we assigned 70% of the total ICU beds to Covid-19 patients. We estimated this ratio from the countries that we have the information about dedicated ICU beds to Covid-19 patients.

Table E.3: LIST OF ESSENTIAL SECTORS DURING LOCKDOWNS

NACE Rev. 2	Definition
01	Crop and animal production, hunting and related service activities
10	Manufacture of food products
1722	Manufacture of household and sanitary goods and of toilet requisites
1811	Printing of newspapers
1920	Manufacture of refined petroleum products
21	Manufacture of basic pharmaceutical products and pharmaceutical preparations
35	Electricity, gas, steam and air conditioning supply
36	Water collection, treatment and supply
463	Wholesale of food, beverages and tobacco
4646	Wholesale of pharmaceutical goods
4711	Retail sale in non-specialised stores with food, beverages or tobacco predominating
472	Retail sale of food, beverages and tobacco in specialised stores
4730	Retail sale of automotive fuel in specialised stores
4773	Dispensing chemist in specialised stores
4774	Retail sale of medical and orthopaedic goods in specialised stores
4781	Retail sale via stalls and markets of food, beverages and tobacco products
4920	Freight rail transport
4941	Freight transport by road
5224	Cargo handling
53	Postal and courier activities
60	Programming and broadcasting activities
61	Telecommunications
639	Other information service activities
75	Veterinary activities
86	Human health activities
87	Residential care activities

NOTES: This table provides the list of the essential sectors that we consider for the implementation of lockdowns under Scenario I & Scenario II. These sectors are identified by the full lockdown practices of countries. Turkish Ministry of Interior, for example, issued a decree on April 10, 2020 indicating the list of essential sectors.

Table E.4: Model-Implied Real Expenditure Losses Relative to the Pre-Pandemic Levels under Scenario II (percent): The Role of Full Lockdowns

	World	Share of AEs (%)	AE	EMDE
Baseline - with lockdowns	0.757	38.8	0.518	1.071
No lockdowns	0.549	38.9	0.377	0.775

NOTES: This table presents model-implied country-level real expenditure losses under Scenario II. AEs follow a vaccination calendar to vaccinate the full population within four months, whereas EMDEs follow a more gradual vaccination calendar, with only half of the population getting vaccinated in one year. The second row recomputes the losses under this baseline scenario, however in this case we do not allow for full lockdowns, which alters the evolution of the pandemic over the course of the year.

F Model Calculations

The notation that we use is summarized in Table F.1.

Table F.1: NOTATION USED IN THE MODEL

Var.	Dimensions	Explanation
C	1	Number of countries.
N (F)	1	Number of industries (factors).
CN (CF)	1	Number of country-industry (country-factor) pairs.
$\Omega^{\mathcal{N}}$	$CN \times CN$	Intermediate input shares.
Ωs	$CN \times N$	Sectoral aggregate input shares (calculated from $\Omega^{\mathcal{N}}$).
Ξ	$CN \times CN$	Sectoral input shares for production.
$\Omega^{\mathcal{F}}$	$CN \times CF$	Factor input shares.
Ω^0	$C \times CN$	Expenditure shares.
$\Omega^0 s$	$C \times N$	Sectoral aggregate expenditure shares.
Ξ^0	$C \times CN$	Sectoral input shares for consumption.
α	$CN \times 1$	Sectoral value-added (VA) shares.
Δ^0	$C \times CN$	Sectoral demand shocks.
Δ^L	$1 \times CN$	Sectoral supply shocks. We also use $d \log L = d \log \Delta^L$
$\Psi^{\mathcal{N}}$	$CN \times CN$	Leontief Inverse for goods: $\Psi^{\mathcal{N}} \equiv (I - \Omega^{\mathcal{N}})^{-1}$.
$\Psi^{\mathcal{F}}$	$CN \times CF$	Leontief Inverse for factors: $\Psi^{\mathcal{F}} \equiv \Psi^{\mathcal{N}} \Omega^{\mathcal{F}}$.
λ	$1 \times CN$	Domar weights for goods.
Λ	$1 \times CF$	Domar weights for factors.
L	$1 \times C$	Factor levels.
χ	$1 \times C$	Expenditure/ Income shares of countries.
p	$1 \times CN$	Good prices.
w	$1 \times CF$	Factor prices.
$\tilde{\varsigma}$	$N \times 1$	Elasticity of substitution (EoS) within sectors for production.
$\tilde{\varsigma}^0$	$N \times 1$	EoS within sectors for consumption.
σ	scalar	Consumption EoS across sectors.
ε	scalar	EoS across input-bundles.
ϕ	scalar	EoS across VA and intermediate input bundle.
1_n	n	Vector of ones of dimension n.
I_n	$n \times n$	Identity Matrix of size n.

Solving for Shocks

Rewriting Equation (15) here:

$$d\Lambda = d\chi\, \Omega^0\, \Psi^{\mathcal{F}} + \chi\, d\Omega^0\, \Psi^{\mathcal{F}} + \lambda\, d\Omega^{\mathcal{N}}\, \Psi^{\mathcal{F}} + \lambda\, d\Omega^{\mathcal{F}}, \tag{F.1}$$

we would like to write each term in terms of $d \log w$. We assume that the labor supply shocks are exogenous and factor level changes satisfy $d \log L = d \log \Delta^L$. The relationship between factor Domar weights and factor wages are given by:

$$d \log \Lambda = d \log w + d \log L \Rightarrow d\Lambda = (d \log w + d \log L)\hat{\Lambda},$$

where $\hat{\Lambda}$ is the diagonal matrix whose diagonal elements are given by Λ. Therefore:

$$d\log w = d\Lambda\hat{\Lambda}^{-1} - d\log L.$$

Also note that, using Shepard Lemma, by transposing both sides in Equation (14), we can write:

$$d\log p = d\log w\,\Psi^{\mathcal{F}'}.$$

Therefore, we can easily write price changes in terms of factor price changes. To solve the model, we will arrive at an equation:

$$d\log w = d\log w\,A + B \quad \Rightarrow \quad d\log w = B\,(I-A)^{-1}.$$

There are four terms in Equation (F.1). We will convert each term $i = 1,2,3,4$ to $d\log w\,A_i + B_i$ format. Then, we will combine all equations to arrive at the solution.

First term: $d\chi\,\Omega^0\,\Psi^{\mathcal{F}}$

For the first term in Equation (F.1), we can use Equation (11) to write the changes in the country income level in terms of the changes in factor Domar weights:

$$d\chi = d\Lambda\,\Phi^E = (d\log w + d\log L)\hat{\Lambda}\,\Phi^E.$$

Therefore, we can write:

$$d\chi\,\Omega^0\,\Psi^{\mathcal{F}} = d\log w\,\underbrace{\hat{\Lambda}\,\Phi^E\,\Omega^0\,\Psi^{\mathcal{F}}}_{A_1} + \underbrace{d\log L\,\hat{\Lambda}\,\Phi^E\,\Omega^0\,\Psi^{\mathcal{F}}}_{B_1}.$$

Second term: $\chi\,d\Omega^0\,\Psi^{\mathcal{F}}$

For the second term, we need to calculate $d\Omega^0$. Each individual term of Ω^0 can be written as:

$$\begin{aligned}\Omega^{0c}_{jm} &= \omega^{0c}_{jm}(\Delta^{0c}_{jm})^{\sigma}\left(\frac{p_{jm}}{p^{0c}_j}\right)^{-\xi^0_i}\left(\frac{p^{0c}_j}{p_{0c}}\right)^{-\sigma}\left(\frac{p_{jm}}{p_{0c}}\right)\\ &= \omega^{0c}_{jm}(\Delta^{0c}_{jm})^{\sigma}\left(p_{jm}\right)^{1-\xi^0_i}\left(p^{0c}_j\right)^{\xi^0_i-\sigma}\left(p_{0c}\right)^{\sigma-1}.\end{aligned}$$

Here, we distinguish between the structural parameters, ω^{0c}_{jm} and observed share Ω^{0c}_{jm}. Before the shocks, we calibrate $\omega^{0c}_{jm} = \Omega^{0c}_{jm}$. We can write the elements of $d\log\Omega^0$ with:

$$d\log\Omega^{0c}_{jm} = \sigma\,d\log\Delta^{0c}_{jm} + (1-\xi^0_i)d\log p_{jm} + (\xi^0_i-\sigma)d\log p^{0c}_j + (\sigma-1)d\log p_{0c}.$$

Using Shepard Lemma, we can write the price index for sectoral consumption bundles with:

$$d\log p_j^{0c} = \sum_{n\in\mathcal{C}} \Xi_{jn}^{0c} d\log p_{jn}^{c}.$$

Similarly:

$$d\log p_{0c} = \sum_{i\in\mathcal{N}} \Omega s_i^{0c} d\log p_i^{0c} = \sum_{i\in\mathcal{N}} \Omega s_i^{0c} \sum_{n\in\mathcal{C}} \Xi_{in}^{0c} d\log p_{in} = \sum_{in\in\mathcal{CN}} \Omega_{in}^{0c} d\log p_{in}.$$

Replacing the corresponding price indices:

$$d\log \Omega_{jm}^{0c} = \sigma\, d\log \Delta_{jm}^{0c} + (1-\xi_j^0) d\log p_{jm} + (\xi_j^0 - \sigma) \sum_{n\in\mathcal{C}} \Xi_{jn}^{0c} d\log p_{jn} + (\sigma-1) \sum_{in\in\mathcal{CN}} \Omega_{in}^{0c} d\log p_{in}.$$

We will write each term in $\chi\, d\Omega^0$ in terms of $d\log p$. Elements of $\chi\, d\Omega^0$ are:

$$\sum_c \chi_c \Omega_{jm}^{0c} d\log \Omega_{jm}^{0c} =$$

Line 1:	$\sigma \sum_c \chi_c \Omega_{jm}^{0c} d\log \Delta_{jm}^{0c}$	$\tilde{B}_{21}$
Line 2:	$+ (1-\xi_j^0) \sum_c \chi_c \Omega_{jm}^{0c} d\log p_{jm}$	$d\log p\, \tilde{A}_{22}$
Line 3:	$+ (\xi_j^0 - \sigma) \sum_c \chi_c \Omega_{jm}^{0c} \sum_{n\in\mathcal{C}} \Xi_{jn}^{0c} d\log p_{jn}$	$d\log p\, \tilde{A}_{23}$
Line 4:	$+ (\sigma-1) \sum_c \chi_c \Omega_{jm}^{0c} \sum_{in\in\mathcal{CN}} \Omega_{in}^{0c} d\log p_{in}$	$d\log p\, \tilde{A}_{24}$

We will convert all $\tilde{A}$ matrices that operate on $d\log p$ to matrices operating on $d\log w$ by multiplying with $\Psi^{\mathcal{F}'}$ on the left. Moreover, to obtain $\chi\, d\Omega^0\, \Psi^{\mathcal{F}}$, we need to multiply all these terms by $\Psi^{\mathcal{F}}$ on the right.

Line 1: The first term does not have any term involving $d\log p$. Therefore, $\tilde{A}_{21} = 0$. The constant term is:

$$B_{21} = \tilde{B}_{21}\, \Psi^{\mathcal{F}} = \sigma\, \chi\, (\Omega^0 \odot d\log \Delta)\, \Psi^{\mathcal{F}},$$

where $\odot$ represents the element-wise (Hadamard) product.

Line 2: jm^{th} element of the second line is given by

$$(d\log p\, \tilde{A}_{22})_{jm} = (1-\xi_j^0) \sum_c \chi_c \Omega_{jm}^{0c} d\log p_{jm}.$$

We can write $\tilde{A}_{22}$ as:

$$\tilde{A}_{22} = (1-\widehat{\xi^0})\, \widehat{\chi\Omega^0}$$

where $\widehat{\xi^0}$ is the diagonal matrix of sectoral elasticities matched to sector-industry combinations and $\widehat{\chi\Omega^0}$ is the diagonal matrix whose elements are given by the vector $\chi\Omega^0$.

Therefore:

$$A_{22} = \Psi^{\mathcal{F}'}\, \tilde{A}_{22}\, \Psi^{\mathcal{F}} = \Psi^{\mathcal{F}'}\, (1 - \widehat{\xi^0})\, \widehat{\chi\Omega^0}\, \Psi^{\mathcal{F}}.$$

Line 3: jm^{th} element of the third line is given by:

$$(d \log p\, \tilde{A}_{23})_{jm} = (\xi_j^0 - \sigma) \sum_c \chi_c \Omega_{jm}^{0c} \sum_{n \in \mathcal{C}} \Xi_{jn}^{0c} d \log p_{jn}.$$

We can write $\tilde{A}_{23}$ as:

$$\tilde{A}_{23} = (\widehat{\xi^0} - \sigma) \left[(1_{C \times C} \otimes I_N) \odot \left(\Xi^{0'}\, \hat{\chi}\, \Omega^0 \right) \right],$$

where $1_{C \times C}$ is the $C \times C$ matrix of ones and $\otimes$ is the Kronecker product operator. $(1_{C \times C} \otimes I_N)$ term is used to select for the sector varieties from different countries. Therefore:

$$A_{23} = \Psi^{\mathcal{F}'}\, \tilde{A}_{23}\, \Psi^{\mathcal{F}} = \Psi^{\mathcal{F}'}\, (\widehat{\xi^0} - \sigma) \left[(1_{C \times C} \otimes I_N) \odot \left(\Xi^{0'}\, \hat{\chi}\, \Omega^0 \right) \right] \Psi^{\mathcal{F}}.$$

Line 4: jm^{th} element of the fourth line is given by

$$(d \log p\, \tilde{A}_{24})_{jm} = (\sigma - 1) \sum_c \chi_c \Omega_{jm}^{0c} \sum_{in \in \mathcal{CN}} \Omega_{in}^{0c} d \log p_{in}.$$

We can write $\tilde{A}_{24}$ as:

$$\tilde{A}_{24} = (\sigma - 1)\, \Omega^{0'}\, \hat{\chi}\, \Omega^0,$$

where $\hat{\chi}$ is the diagonal matrix whose diagonal elements are given by χ. Therefore:

$$A_{24} = \Psi^{\mathcal{F}'}\, \tilde{A}_{24}\, \Psi^{\mathcal{F}} = (\sigma - 1)\, \Psi^{\mathcal{F}'}\, \Omega^{0'}\, \hat{\chi}\, \Omega^0\, \Psi^{\mathcal{F}}.$$

Third term: $\lambda\, d\Omega^{\mathcal{N}}\, \Psi^{\mathcal{F}}$

Many of the calculations are similar to the second term, so we will skip some of the steps. We need to calculate $d\Omega^{\mathcal{N}}$ for the third term:

$$\begin{aligned}
\Omega_{jm}^{kc} &= \omega_{jm}^{kc} \left(\frac{p_{jm}}{p_j^{kc}} \right)^{-\xi_j} \left(\frac{p_j^{kc}}{p_M^{kc}} \right)^{-\varepsilon} \left(\frac{p_M^{kc}}{p_{kc}} \right)^{-\phi} \left(\frac{p_{jm}}{p_{kc}} \right) \\
&= \omega_{jm}^{kc} \left(p_{jm} \right)^{1-\xi_j} \left(p_j^{kc} \right)^{\xi_j - \varepsilon} \left(p_{M_{kc}} \right)^{\varepsilon - \phi} \left(p_{kc} \right)^{\phi - 1}.
\end{aligned}$$

Again, we distinguish between the structural parameters, ω_{jm}^{kc} and observed share Ω_{jm}^{kc}. Before the shocks, we calibrate $\omega_{jm}^{kc} = \Omega_{jm}^{kc}$. We can write the elements of $d\log\Omega^{\mathcal{N}}$ as:

$$d\log\Omega_{jm}^{kc} = (1-\xi_j)d\log p_{jm} + (\xi_j - \varepsilon)\sum_{n\in\mathcal{C}}\Xi_{jn}^{0c}d\log p_{jn} + (\varepsilon-\phi)\sum_{in\in\mathcal{CN}}\frac{\Omega_{in}^{kc}}{1-\alpha_{kc}}d\log p_{in} + (\phi-1)d\log p_{kc}.$$

We will write each term in $\lambda\, d\Omega^{\mathcal{N}}$ in terms of $d\log p$. Elements of $\lambda\, d\Omega^{\mathcal{N}}$ are:

$$\sum_{kc\in\mathcal{CN}}\lambda_{kc}\Omega_{jm}^{kc}d\log\Omega_{jm}^{kc} =$$

Line 1:	$\sum_{kc\in\mathcal{CN}}\lambda_{kc}\Omega_{jm}^{kc}(1-\xi_j)d\log p_{jm}$	$d\log p\,\tilde{A}_{31}$
Line 2:	$+(\xi_j-\varepsilon)\sum_{kc\in\mathcal{CN}}\lambda_{kc}\Omega_{jm}^{kc}\sum_{n\in\mathcal{C}}\Xi_{jn}^{kc}d\log p_{jn}$	$d\log p\,\tilde{A}_{32}$
Line 3:	$+(\varepsilon-\phi)\sum_{kc\in\mathcal{CN}}\lambda_{kc}\Omega_{jm}^{kc}\sum_{in\in\mathcal{CN}}\frac{\Omega_{in}^{kc}}{1-\alpha_{kc}}d\log p_{in}$	$d\log p\,\tilde{A}_{33}$
Line 4:	$+(\phi-1)\sum_{kc\in\mathcal{CN}}\lambda_{kc}\Omega_{jm}^{kc}d\log p_{kc}$	$d\log p\,\tilde{A}_{34}$.

Line 1: jm^{th} element of the first line is given by

$$(d\log p\,\tilde{A}_{31})_{jm} = \sum_{kc\in\mathcal{CN}}\lambda_{kc}\Omega_{jm}^{kc}(1-\xi_j)d\log p_{jm}.$$

We can write $\tilde{A}_{31}$ as:

$$\tilde{A}_{31} = (1-\hat{\xi})\,\widehat{\lambda\Omega^{\mathcal{N}}}$$

where $\hat{\xi}$ is the diagonal matrix of sectoral elasticities matched to sector-industry combinations and $\widehat{\lambda\Omega^{\mathcal{N}}}$ is the diagonal matrix whose elements are given by the vector $\lambda\Omega^{\mathcal{N}}$. Therefore:

$$A_{31} = \Psi^{\mathcal{F}'}\,\tilde{A}_{31}\,\Psi^{\mathcal{F}} = \Psi^{\mathcal{F}'}\,(1-\hat{\xi})\,\widehat{\lambda\Omega^{\mathcal{N}}}\,\Psi^{\mathcal{F}}.$$

Line 2: jm^{th} element of the second line is given by:

$$(d\log p\,\tilde{A}_{32})_{jm} = (\xi_j-\varepsilon)\sum_{kc\in\mathcal{CN}}\lambda_{kc}\Omega_{jm}^{kc}\sum_{n\in\mathcal{C}}\Xi_{jn}^{kc}d\log p_{jn}.$$

We can write $\tilde{A}_{23}$ as:

$$\tilde{A}_{32} = (\hat{\xi}-\varepsilon)\left[(1_{C\times C}\otimes I_N)\odot\left(\Xi^{\mathcal{N}'}\,\hat{\lambda}\,\Omega^{\mathcal{N}}\right)\right],$$

where $1_{C\times C}$ is the $C\times C$ matrix of ones and $\otimes$ is the Kronecker product operator.

$(1_{C\times C} \otimes I_N)$ term is used to select the sector varieties from different countries. Therefore:

$$A_{32} = \Psi^{\mathcal{F}'}\, \tilde{A}_{32}\, \Psi^{\mathcal{F}} = \Psi^{\mathcal{F}'}\, (\hat{\xi} - \varepsilon)\, \left[(1_{C\times C} \otimes I_N) \odot \left(\Xi^{\mathcal{N}'}\, \hat{\lambda}\, \Omega^{\mathcal{N}} \right) \right]\, \Psi^{\mathcal{F}}.$$

Line 3: jm^{th} element of the third line is given by

$$(d\log p\, \tilde{A}_{33})_{jm} = (\varepsilon - \phi) \sum_{kc\in\mathcal{CN}} \lambda_{kc} \Omega^{kc}_{jm} \sum_{in\in\mathcal{CN}} \frac{\Omega^{kc}_{in}}{1-\alpha_{kc}} d\log p_{in}.$$

We can write $\tilde{A}_{33}$ as:

$$\tilde{A}_{33} = (\varepsilon - \phi)\, \Omega^{\mathcal{N}'}\, \hat{\lambda}\, (1-\hat{\alpha})^{-1}\, \Omega^{\mathcal{N}},$$

where $\hat{\lambda}$ is the diagonal matrix whose diagonal elements are given by λ and $\hat{\alpha}$ is the diagonal matrix whose elements are the value-added shares. Therefore:

$$A_{33} = \Psi^{\mathcal{F}'}\, \tilde{A}_{33}\, \Psi^{\mathcal{F}} = (\varepsilon - \phi)\, \Psi^{\mathcal{F}'}\, \Omega^{\mathcal{N}'}\, \hat{\lambda}\, (1-\hat{\alpha})^{-1}\, \Omega^{\mathcal{N}}\, \Psi^{\mathcal{F}}.$$

Line 4: jm^{th} element of the fourth line is given by

$$(d\log p\, \tilde{A}_{34})_{jm} = (\phi - 1) \sum_{kc\in\mathcal{CN}} \lambda_{kc} \Omega^{kc}_{jm} d\log p_{kc}.$$

We can write $\tilde{A}_{34}$ as:

$$\tilde{A}_{34} = (\phi - 1)\hat{\lambda}\, \Omega^{\mathcal{N}}.$$

Therefore:

$$A_{34} = \Psi^{\mathcal{F}'}\, \tilde{A}_{34}\, \Psi^{\mathcal{F}} = (\phi - 1)\, \Psi^{\mathcal{F}'}\, \hat{\lambda}\, \Omega^{\mathcal{N}}\, \Psi^{\mathcal{F}}.$$

Fourth term: $\lambda\, d\Omega^{\mathcal{F}}$

For the fourth term, we start with the individual factor terms:

$$\begin{aligned}
\Omega^{kc}_{f} &= \omega^{kc}_{f} \left(\frac{w_f}{p^{kc}_{VA}} \right)^{-\eta} \left(\frac{p^{kc}_{VA}}{p_{kc}} \right)^{-\phi} \left(\frac{w_f}{p_{kc}} \right) \\
&= \omega^{kc}_{fm} \left(w_f \right)^{1-\eta} \left(p^{kc}_{VA} \right)^{\eta-\phi} \left(p_{kc} \right)^{\phi-1}.
\end{aligned}$$

Again, we distinguish between the structural parameters, ω^{kc}_{f} and observed share Ω^{kc}_{f}. Before the shocks, we calibrate $\omega^{kc}_{f} = \Omega^{kc}_{f}$. We can write the elements of $d\log\Omega^{\mathcal{F}}$ as:

$$d\log\Omega^{kc}_{f} = (1-\eta) d\log w_f + (\eta - \phi) \sum_{g\in\mathcal{F}} \frac{\Omega^{kc}_{g}}{\alpha_{kc}} d\log w_g + (\phi - 1) d\log p_{kc}.$$

We will write each term in $\lambda\, d\Omega^{\mathcal{F}}$ in terms of $d\log w$ and $d\log p$. Elements of $\lambda\, d\Omega^{\mathcal{F}}$ are:

$$\sum_{kc\in\mathcal{CN}} \lambda_{kc}\Omega_f^{kc} d\log\Omega_f^{kc} =$$

$$\begin{aligned}
&\text{Line 1:} && (1-\eta) d\log w_f \sum_{kc\in\mathcal{CN}} \lambda_{kc}\Omega_f^{kc} && d\log w\, A_{41}\\
&\text{Line 2:} && +(\eta-\phi)\sum_{kc\in\mathcal{CN}} \lambda_{kc}\Omega_f^{kc}\sum_{g\in\mathcal{F}}\frac{\Omega_g^{kc}}{\alpha_{kc}} d\log w_g && d\log w\, A_{42}\\
&\text{Line 3:} && +(\phi-1)\sum_{kc\in\mathcal{CN}} \lambda_{kc}\Omega_f^{kc} d\log p_{kc} && d\log p\, \tilde{A}_{43}.
\end{aligned}$$

Line 1: f^{th} element of the first line is given by

$$(d\log w\, A_{41})_f = (1-\eta) d\log w_f \sum_{kc\in\mathcal{CN}} \lambda_{kc}\Omega_f^{kc}.$$

We can write A_{41} as:

$$A_{41} = (1-\eta)\widehat{\lambda\Omega^{\mathcal{F}}}$$

where $\widehat{\lambda\Omega^{\mathcal{F}}}$ is the diagonal matrix whose elements are given by the vector $(\lambda\Omega^{\mathcal{F}})$.

Line 2: f^{th} element of the second line is given by

$$(d\log w\, A_{42})_f = (\eta-\phi)\sum_{kc\in\mathcal{CN}} \lambda_{kc}\Omega_f^{kc}\sum_{g\in\mathcal{F}}\frac{\Omega_g^{kc}}{\alpha_{kc}} d\log w_g.$$

We can write A_{42} as:

$$A_{42} = (\eta-\phi)\,\Omega^{\mathcal{F}'}\,\hat{\lambda}\,\hat{\alpha}^{-1}\,\Omega^{\mathcal{F}},$$

where $\hat{\lambda}$ is the diagonal matrix whose diagonal elements are given by λ and $\hat{\alpha}$ is the diagonal matrix whose elements are the value-added shares

Line 3: jm^{th} element of the third line is given by

$$(d\log p\, \tilde{A}_{33})_{jm} = (\phi-1)\sum_{kc\in\mathcal{CN}} \lambda_{kc}\Omega_f^{kc} d\log p_{kc}.$$

We can write $\tilde{A}_{33}$ as:

$$\tilde{A}_{33} = (\phi-1)\hat{\lambda}\,\Omega^{\mathcal{F}}$$

Therefore:

$$A_{43} = \Psi^{\mathcal{F}'}\,\tilde{A}_{43} = (\phi-1)\,\Psi^{\mathcal{F}'}\,\hat{\lambda}\,\Omega^{\mathcal{F}}.$$

Sanity Check

If all the calculations are correct, the resultant A matrix should be singular because of redundancies. Therefore, we need to replace one of the conditions with the fact that the world nominal GDP is constant:

$$dE = \sum_f d\lambda_f = \sum_g \lambda_f (d \log w_f + d \log L_f) = 0.$$

Hence, we can use this relation to break the singularity:

$$A_{1,1} = 0, \quad A_{f>1,1} = -\Lambda_f \quad \text{and} \quad B_1 = -\log L \cdot \Lambda'.$$

Updating Variables

After solving for $d \log w_g$, we can solve for other variables as follows.

Good Prices: Using Shepard Lemma, we can easily obtain good prices with:

$$d \log p' = \Psi^{\mathcal{F}} d \log w'$$

Factor Domar Weights are related to the factor wages with:

$$d\Lambda = \hat{\Lambda}(d \log w + d \log L).$$

Country Income Shares:

$$d\chi = d\Lambda \, \Phi^E.$$

Changes in consumption patterns:

$$d \log \Omega^{0c}_{jm} = \sigma \, d \log \Delta^{0c}_{jm} + (1 - \xi_j) d \log p_{jm} + (\xi_j - \sigma) \sum_{n \in \mathcal{C}} \Xi^{0c}_{jn} d \log p_{jn} + (\sigma - 1) \sum_{in \in \mathcal{CN}} \Omega^{0c}_{in} d \log p_{in}.$$

Each term is given by:

- $\sigma \, d \log \Delta^{0c}_{jm}$ term in matrix notation:

$$\sigma \, d \log \Delta$$

- $(1 - \xi^0_j) d \log p_{jm}$ term in matrix notation:

$$(d \log p \otimes 1_C) \, (I - \widehat{\xi^0})$$

- $(\xi^0_j - \sigma) \sum_{n \in \mathcal{C}} \Xi^{0c}_{jn} d \log p_{jn}$ term:

$$1'_C \otimes ([(d \log p \otimes 1_C) \odot \Xi^0](\widehat{\xi^0} - \sigma) \, \Sigma^{\mathcal{N}}),$$

where $\Sigma^{\mathcal{N}}$ matrix sums the country varieties.

- $(\sigma - 1) \sum_{in \in \mathcal{CN}} \Omega_{in}^{0c} d \log p_{in}$ term:

$$(\sigma - 1)([(d \log p \otimes 1_C) \odot \Omega^0] \, 1_{CN}) \otimes 1'_{CN}.$$

Finally:

$$d\Omega^0 = \Omega^0 \odot d \log \Omega^0$$

Changes in input weights: We can write the changes in elements of $d \log \Omega^{\mathcal{N}}$:

$$\begin{aligned} d \log \Omega_{jm}^{kc} = & (1 - \xi_j) d \log p_{jm} \\ & + (\xi_j - \varepsilon) \sum_{n \in \mathcal{C}} \Xi_{jn}^{0c} d \log p_{jn} \\ & + (\varepsilon - \phi) \sum_{in \in \mathcal{CN}} \frac{\Omega_{in}^{kc}}{1 - \alpha_{kc}} d \log p_{in} \\ & + (\phi - 1) d \log p_{kc}. \end{aligned}$$

Each element is given by:

- $(1 - \xi_j) d \log p_{jm}$ term in matrix notation:

$$(d \log p \otimes 1_{CN}) \, (I - \hat{\xi})$$

- $(\xi_j - \varepsilon) \sum_{n \in \mathcal{C}} \Xi_{jn}^{kc} d \log p_{jn}$ term:

$$1'_C \otimes ([(d \log p \otimes 1_{CN}) \odot \Xi^{\mathcal{N}}](\hat{\xi} - \sigma) \, \Sigma^{\mathcal{N}}).$$

- $(\varepsilon - \phi) \sum_{in \in \mathcal{CN}} \frac{\Omega_{in}^{kc}}{1 - \alpha_{kc}} d \log p_{in}$ term:

$$(\varepsilon - \phi) \, (1 - \hat{\alpha})^{-1} \, \Omega^{\mathcal{N}} \, (d \log p \otimes 1_{CN}).$$

- $(\phi - 1) d \log p_{kc}$ term:

$$(\phi - 1)(d \log p' \otimes 1'_{CN}).$$

Finally:

$$d\Omega^{\mathcal{N}} = \Omega^{\mathcal{N}} \odot d \log \Omega^{\mathcal{N}}$$

Changes in factor shares: Factor share change terms are given by:

$$\begin{aligned} d \log \Omega_f^{kc} = & (1 - \eta) d \log w_f \\ & + (\eta - \phi) \sum_{g \in \mathcal{F}} \frac{\Omega_g^{kc}}{\alpha_{kc}} d \log w_g \end{aligned}$$

$$+ (\phi - 1) d \log p_{kc}.$$

Each element is given by

- $(1-\eta) d \log w_f$ term in matrix notation:

$$(1-\eta)(1_{CN} \otimes d \log w)$$

- $(\eta - \phi) \sum_{g \in \mathcal{F}} \frac{\Omega_g^{kc}}{\alpha_{kc}} d \log w_g$ term:

$$(\eta - \phi)[\hat{\alpha}^{-1} \, \Omega^{\mathcal{F}} \, d \log w'] \otimes 1'_{CF}.$$

- $(\phi - 1) d \log p_{kc}$:

$$(\phi - 1)(d \log p' \otimes 1'_{CF}).$$

Finally:

$$d\Omega^{\mathcal{F}} = \Omega^{\mathcal{F}} \odot d \log \Omega^{\mathcal{F}}$$

Leontief Inverse: We can write $d\Psi^{\mathcal{N}}$ as:

$$d \, \Psi^{\mathcal{N}} = \Psi^{\mathcal{N}} \, d\Omega^{\mathcal{N}} \, \Psi^{\mathcal{N}}.$$

Good Domar Weights:

$$d\lambda = (d\chi \, \Omega^0 + \chi \, \Omega^0 + \lambda \, d\Omega^{\mathcal{N}}) \, \Psi^{\mathcal{N}}.$$